



**Final Report** 

Strong exciton-photon coupling regime and Polariton properties

in quantuwm well microcavity

By Kanchana Sivalertporn

## **Final Report**

## Strong exciton-photon coupling regime and Polariton properties

in quantuwm well microcavity

Kanchana Sivalertporn Ubonratchathani University

#### **Abstract**

Project Code: MRG6180073

Project Title: Strong exciton-photon coupling regime and Polariton properties in quantum well

microcavity

Investigator: Kanchana Sivalertporn

E-mail Address : kanchana.s@ubu.ac.th

Project Period: 2 years

## บทคัดย่อ

ในการวิจัยนี้ได้ทำการศึกษาเชิงทฤษฎีเกี่ยวกับสถานะพลังงานของเอ็กซิตอน (Exciton) ในโครงสร้าง บ่อศักย์ควอนดัมแบบเดี่ยวและแบบคู่ โดยพิจารณาทั้งผลของความกว้างชั้นบ่อศักย์ต่างๆ ความลึกของศักย์ รูปร่างของบ่อศักย์ และสนามไฟฟ้าภายนอกที่มีต่อระดับพลังงานของอิเล็กตรอนและโฮล และเลือกใช้ พารามิเตอร์ของวัสดุ GaAs/AlGaAs และ GalnNAs/GaAs ซึ่งเป็นวัสดุที่ถูกนำมาประยุกต์ใช้งานอย่าง กว้างขวาง ในกรณีของโครงสร้างบ่อศักย์ควอนดัมคู่ GalnNAs/GaAs พบว่า สถานะพื้นของเอ็กซิตอนมีการ เปลี่ยนจากเอ็กซิตอนแบบตรง (Direct exciton) เป็นแบบไม่ตรง (Indirect exciton) ที่ค่าสนามไฟฟ้า 12 kV/cm นอกจากนี้ยังได้ทำการศึกษาเชิงทฤษฎีเกี่ยวกับอันตรกิริยาระหว่างเอ็กซิตอนและโฟตอนใน โครงสร้างไมโครคาวิตี้แบบบ่อศักย์ควอนดัม โดยใช้โครงสร้างบ่อศักย์ควอนดัมคู่ GalnNAs/GaAs ที่มีความ กว้างของบ่อศักย์ค่าต่างๆ จากการศึกษากรณีบ่อศักย์ 8-5-10-nm GalnNAs/GaAs และพลังงานโฟตอนที่ 1.411 eV พบสถานะโพลาริตอนที่ประกอบด้วยสัดส่วนของเอ็กซิตอนแบบไม่ตรงและโฟตอนเท่ากับ 0.4 และเอ็กซิตอนแบบตรง 0.2 นั่นแสดงว่า สถานะโพลาริตอนนี้จะได้รับสมบัติของทั้งเอ็กซิตอนแบบตรงและ แบบไม่ตรง จึงทำให้เป็นสถานะโพลาริตอนที่มีค่าไดโพลโมเมนต์สูงเนื่องจากได้รับสมบัตินี้จากเอ็กซิตอนแบบไม่ตรงนั่นเอง

Abstract:

Semiconductor microcavities are well known due to their importance in fundamental physics

and have a wide range of various applications. The system consists of the GalnNAs/GaAs double

quantum wells embedded in a planar Bragg-mirror microcavity. The polariton can be formed due to

the exciton-photon coupling in the microcavity. The direct exciton with large oscillator strength

strongly couples to the cavity mode. The indirect exciton with small oscillator strength can interact

with photon via the direct exciton since it is electronically coupled to the direct exciton. The polariton

state and its fractions (direct exciton, indirect exciton and photon) are calculated as a function of

applied electric field. The strong-weak coupling regime is controlled by the applied electric field. The

dipolariton state with comparable components is observed at approximately F=12 kV/cm where the

photon strongly couple to the exciton ground state and the ground state exhibits the direct-indirect

anticrossing also. This mixed state acquires large oscillator strength from the direct exciton and large

electric dipole moment from the indirect exciton.

Keywords: Exciton, Polariton, Light-matter coupling, Quantum well, Microcavity

#### 1. Abstract

Semiconductor microcavities are well known due to their importance in fundamental physics and have a wide range of various applications. The system consists of the GalnNAs/GaAs double quantum wells embedded in a planar Bragg-mirror microcavity. The polariton can be formed due to the exciton-photon coupling in the microcavity. The direct exciton with large oscillator strength strongly couples to the cavity mode. The indirect exciton with small oscillator strength can interact with photon via the direct exciton since it is electronically coupled to the direct exciton. The polariton state and its fractions (direct exciton, indirect exciton and photon) are calculated as a function of applied electric field. The strong-weak coupling regime is controlled by the applied electric field. The dipolariton state with comparable components is observed at approximately F=12 kV/cm where the photon strongly couple to the exciton ground state and the ground state exhibits the direct-indirect anticrossing also. This mixed state acquires large oscillator strength from the direct exciton and large electric dipole moment from the indirect exciton.

## 2. Executive summary

The coupled quantum well (CQW) structure consists of two QWs separated by a barrier layer as shown in Fig. 1(a). For a sufficiently thin barrier, the tunneling of carriers through the barrier makes the two QWs electronically coupled to each other. As a result, an electron and a hole can either reside in one of the two QWs or their wave functions are distributed between both QWs. In the case of the Coulomb bound electron and hole residing in the same QW, they form a direct exciton. If they are located in different QWs, an indirect exciton is created. A small overlap integral of indirect exciton leads to a longer exciton lifetime compared to that in SQWs. The binding energy also reduces due to the large separation of carriers.

## CQW exciton in the presence of electric field

In a symmetric CQW structure with no electric field applied, the tunneling through the middle barrier causes the splitting of the degenerate single-particle states into doublets with symmetric and antisymmetric states in each. Only the transitions between states having the same parity are optically allowed because the integral of the wave function overlap is nonzero. The Coulomb-coupled e-h pairs form the excitonic states that are optically either bright or dark. When electric field is applied in the growth direction [Fig. 1(b)], it breaks down the symmetry of the system making all these excitons bright. The transition from states with well-defined parity to the ones with the electron

(hole) located in one of the two QWs can form combinations of direct and indirect uncorrelated e-h pair states. These different pair states are Coulomb coupled with each other and form an exciton in which the direct or indirect pair can dominate.

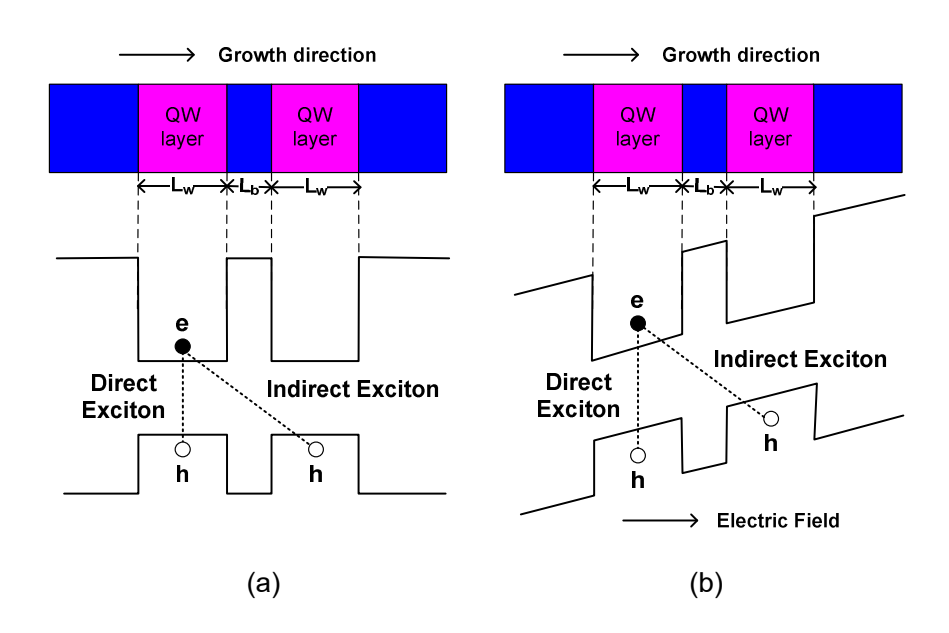


Fig.1: Energy band diagram of a coupled quantum well structure consisting of two QW layers separated by a thin barrier in (a) no field and (b) the presence of electric field.

#### Semiconductor Microcavity

A typical semiconductor microcavity consists of a cavity layer sandwiched between two distributed Bragg reflectors (DBRs) as shown in Fig. 2(a). A DBR is usually made of alternating  $\lambda/4$  layers of different semiconductor materials, with high and low refractive indices. The incident light is reflected at the DBR interface and only a single wavelength, namely that as a cavity mode, is transmitted (indicated as a sharp peak in the reflectivity spectra). This creates also a stop-band in the transmission spectrum. Hence, the DBR behaves as a high reflective mirror for wavelengths within the stop-band. When the quantum confined structure is embedded in the cavity, an exciton in such a structure can interact with a photon inside the cavity and forms an exciton-photon quasiparticle called a polariton. An exciton mode coupled to one photon gives rise to two polariton modes (double peaks are seen in the reflectivity spectra). The lower energy mode is called lower polariton (LP) branch, while the upper polariton (UP) branch refers to the mode with higher energy. In the strong coupling regime, the photon is bounced back and forth between the two DBR mirrors and is absorbed by an exciton. The excited exciton then emits a photon into the cavity by the

radiative emission. The whole sequence of absorption and emission takes place until the photon leaks out from the cavity with decay rate of  $\gamma_{c}$  or the exciton decays through the non-radiative channel by the rate  $\gamma_{x}$  [Fig. 2(b)]. The energy exchange between the exciton and photon is a reversible process, known as the Rabi oscillation. The two polariton energies are given by

$$E_{1,2} = \frac{\omega_{c} + \omega_{x}}{2} - i \frac{\gamma_{c} + \gamma_{x}}{2} \pm \sqrt{\left(\frac{\omega_{c} + i\gamma_{c} - \omega_{x} - i\gamma_{x}}{2}\right)^{2} + g^{2}}$$

where  $\omega_{x}$ ,  $\omega_{c}$  are the uncoupled cavity and exciton mode energies and g is the exciton-photon coupling.

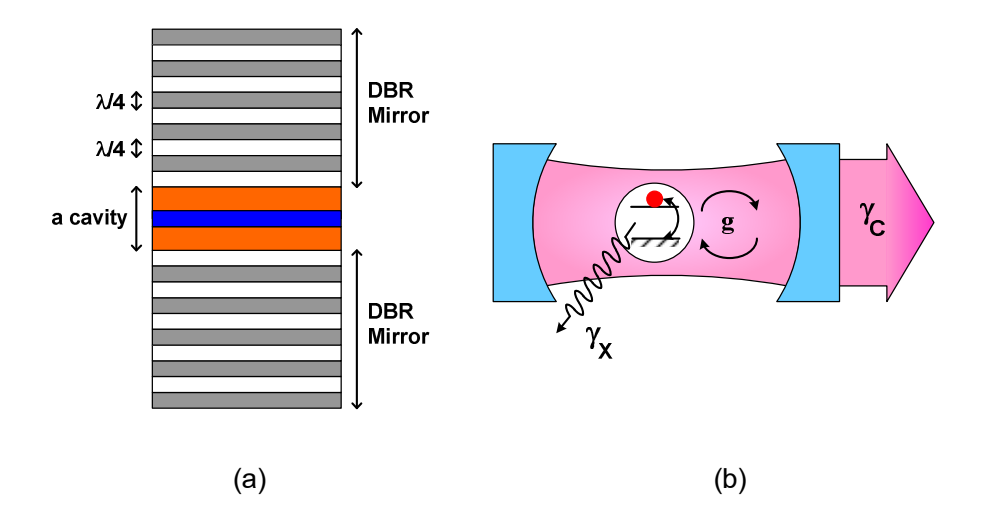


Fig.2: (a) Sketch of a semiconductor microcavity, (b) Schematic of a single two-level atom coupled to a single photon in a cavity.

In the weak coupling regime (g<  $\gamma_{c}$ ,  $\gamma_{x}$ ), the real part of the energies  $E_{1,2}$  are degenerate at zero detuning when the exciton mode is tuned to the cavity mode, corresponding to the crossing of the exciton and photon modes. In this case, the exciton decays well before any re-absorption/re-emission. The decay rate of irreversible emission can be enhanced by the Purcell effect.

#### Literature review

An exciton is a combined state of electron in the conduction band and hole in the valence band bound via the Coulomb interaction. Excitons in a quantum well (QW) are an attractive system for investigation due to their potential applications in electro-optic and optoelectronic devices. Their electronic and optical properties have been studied both experimentally and theoretically in the past decade. In particular, an indirect exciton - a bound state of the electron and hole residing in different QW layers - exists in couple quantum well (CQW) structures in the presence of the electric field perpendicular to the QW layer. A large spatial separation between electron and hole gives rise to a long radiative lifetime of the indirect exciton [1–5].

Semiconductor microcavities are well known due to their importance in fundamental physics and have a wide range of various applications [6]. Of particular interest is exciton polaritons created in microcavities in the regime of strong light-matter coupling [7]. The demonstrated possibilities of polariton condensation [8, 9] and room-temperature lasing [10-12] have made microcavity polaritons the subject of intensive studies. If a semiconductor QW is placed in the antinode position of the resonant electro-magnetic field inside the microcavity, Coulomb bound electrons and holes localized in the QW layer can strongly interact with a high-quality cavity mode and form mixed exciton-photon states called polaritons. Double QWs have attracted much attention in recent years due to formation of long-living spatially indirect excitons in such structures in the presence of an applied electric field [13]. Intensive studies of indirect excitons in double QWs have resulted in demonstration of their electrostatic [14, 15] and optical control [16] as well as in engineering of the dipolar exciton-exciton interaction [17-19] necessary for exploring different many body effects, including an intriguing possibility of Bose-Einstein condensation of excitons [13, 14, 20-22]. Recently, the optical properties of exciton and polariton states have been theoretically and experimentally investigated for different condition [23-25]. The strong coupling regime is also observed [26, 27]. In the previous study [28], we presented a microscopic calculation of the optical spectra of InGaAs quantum well embedded in GaAs microcavity. The results demonstrated the absence of dark polariton states which is claimed by the other works [28, 29]. We also showed in particular that the claimed polariton darkness, or vanishing DX contribution, is an artifact of the basis truncation and neglect of the electron-hole (e-h) relative motion. Here, we will develop the model and study the effect of electric field and structural parameters on the exciton and polariton optical properties.

In this work, the exciton energy and wave function in quantum well (QW) structure are theoretically calculated for different applied electric fields. The single-particle (electron and hole) states in the growth direction are calculated by solving the Schrodinger equation in real space. The

effect of structural parameters such as well width, potential shape and height on the electron and hole energies have also been studied by considering the squared, step and tilted single quantum well structures. The parameters of GaAs/AlGaAs and GalnNAs/GaAs QWs are used in the calculation. For the coupled quantum wells, two types of exciton can be formed: (i) Direct exciton (DX) when an electron and a hole are in the same well and (ii) Indirect exciton (IX) if they are in different well. The direct exciton state has large oscillator strength due to a large overlap of electron and hole wave functions, while the indirect exciton state has large dipole moment since the electron and hole occupy in different well. When applied the electric field to the growth direction, the ground state exciton exhibits the switching of direct to indirect exciton. The GalnNAs/GaAs CQWs are placed in the microcavity in order to study the exciton and photon interaction. The direct exciton strongly couples to the cavity mode and creates a polariton. The indirect exciton itself does not form a polariton, as it has much smaller oscillator strength, but it is electronically coupled to the direct exciton via the tunneling across the barrier. A resulting mixed state of such a three-level system is a dipolariton state. The fraction of direct and indirect excitons and cavity mode are calculated as a function of electric field.

#### References:

- [1] C. C. Phillips, R. Eccleston, and S. R. Andrews, *Phys. Rev. B* 40, 9760 (1989).
- [2] S. C. Arapan and M. A. Liberman, J. Lumin. 112, 216 (2005).
- [3] S. Charbonneau, M. L. W. Thewalt, E. S. Koteles, and B. Elman, *Phys. Rev. B* 38, 6287 (1988).
- [4] J. E. Golub, K. Kash, J. P. Harbison, and L. T. Florez, *Phys. Rev. B* 41, 8564 (1990).
- [5] A. Alexandrou et al., Phys. Rev. B 42, 9225 (1990).
- [6] A. V. Kavokin, J. J. Baumberg, G. Malpuech, and F. P. Laussy, *Microcavities* (Oxford University Press, Oxford, 2007).
- [7] C. Weisbuch, M. Nishioka, A. Ishikawa and Y. Arakawa, Phys. Rev. Lett. 69, 3314 (1992).
- [8] H. Deng et al., Science 298, 199 (2002).
- [9] J. Kasprzak et al., Nature 443, 409 (2006).
- [10] S. Christopoulos et al., Phys. Rev. Lett. 98, 126405 (2007).
- [11] D. Bajoni et al., Phys. Rev. Lett. 100, 047401 (2008).
- [12] G. Christmann et al., Appl. Phys. Lett. 93, 051102 (2008).
- [13] L. V. Butov et al., Nature 417, 47 (2002).
- [14] Z. V"or"os, D. W. Snoke, L. Pfeiffer, and K. West, Phys. Rev. Lett. 97, 016803 (2006).

- [15] A. G. Winbow et al., Phys. Rev. Lett. 106, 196806 (2011).
- [16] G. Grosso et al., Nature Photonics 3, 577 (2009).
- [17] R. Rapaport et al., Phys. Rev. B 72, 075428 (2005).
- [18] C. Schindler and R. Zimmermann, Phys. Rev. B 78, 045313 (2008).
- [19] K. Cohen, R. Rapaport, and P. V. Santos, Phys. Rev. Lett. 106, 126402 (2011).
- [20] S. Yang et al., Phys. Rev. Lett. 97, 187402 (2006).
- [21] V. B. Timofeev and A. V. Gorbunov, J. Appl. Phys. 101, 081708 (2007).
- [22] A. A. High et al., Nature, 483, 584 (2012).
- [23] C. Schmeider et al., Nature. 497, 348 (2013).
- [24] I. Fraj et.al., Curr. Appl. Phys. 17, 1 (2017).
- [25] S. Brodbect et.al., Phys. Rev. Lett. 117, 127401 (2016).
- [26] S. V. Poltavtsev et.al., Phys. Rev. B 89, 081304 (2014).
- [27] A. Tzimis et.al., Appl. Phys. Lett. 107, 101101 (2015).
- [28] K. Sivalertporn and E.A. Muljarov, Phys. Rev. Lett. 115, 117401 (2015).
- [29] G. Christmann et.al., Phys. Rev. B 82, 113308 (2010).
- [30] G. Christmann et.al., Appl. Phys. Lett. 98, 081111 (2011).
- [31] P. Mahala, S. Singh and C. Dhanavantri, Optik 166 61-8 (2018).
- [32] A. Aissat A et.al., Int. J. Hydrog. Energy 42 8790–4 (2017).
- [33] H. Urabe et.al., J. Cryst. Growth 425 330-2 (2015).
- [34] P. Poopanya and K. Sivalertporn, Phys. Lett. A 382 734-8 (2018).
- [35] H. Yıldırım, Superlattice Microst. 114 207–13 (2018).
- [36] M. Arulmozhi and A. Anitha, Superlattice Microst.75 222-32 (2014).
- [37] K. Sivalertporn, Phys. Lett. A 380 1990-4 (2016).
- [38] A. S. Abdalla et.al., Optik 170 314-20 (2018).
- [39] O. Ozturk, E. Ozturk and S. Elagoz, J. Mol. Struct. 1156 726-32 (2018).
- [40] P. S. Grigoryev et.al., Superlattice Microst. 97 452–62 (2016).
- [41] K. Sivalertporn et.al., Phys. Rev. B 85 045207 (2012).
- [42] U. Yesilgul et.al., Physica B 475 110-6 (2015).
- [43] H. M. Khalil et.al., Mater. Sci. Eng. B 177 729-33 (2012).

## 3. Objective

- 3.1 To theoretically study the electrical and optical properties of exciton states in double quantum well structure by the efficient model.
- 3.2 To theoretically study the exciton-photon interaction in quantum well microcavity.
- 3.3 To obtain the basic understanding to explain the phenomena in quantum well microcavity.
- 3.4 To incorporate the research to undergraduate and postgraduate students in terms of special project and thesis, respectively.

## 4. Research methodology

In the effective mass approximation, the excitonic Hamiltonian can be divided into three parts: the first two,  $\hat{H}_e$  and  $\hat{H}_h$ , take into account the electron and hole quantization in heterostructure potentials  $V_e$  and  $V_h$  and the third one,  $\hat{H}_\chi$ , is responsible for the e-h in-plane ( $\rho$ ) relative motion and Coulomb binding:

$$\begin{split} \hat{H}_{ex}(z_{e}, z_{h}, \rho) &= \hat{H}_{e}(z_{e}) + \hat{H}_{h}(z_{h}) + \hat{H}_{x}(z_{e}, z_{h}, \rho) + E_{g}, \\ \hat{H}_{e(h)}(z_{e(h)}) &= -\frac{\hbar}{2m_{e(h)}} \frac{\partial^{2}}{\partial z^{2}} + V_{e(h)} \\ \hat{H}_{x}(z_{e}, z_{h}, \rho) &= -\frac{\hbar^{2}}{2\mu} \left( \frac{\partial^{2}}{\partial \rho^{2}} + \frac{1}{\rho} \frac{\partial}{\partial \rho} \right) + \sum_{m=1}^{N} V_{nm}(\rho) \phi_{m}(\rho) = E_{x} - E_{n}^{(0)}, \\ E_{n}^{(0)} &= E_{e}^{i} + E_{h}^{j} + E_{g}. \end{split}$$

The exciton wave function is written into a finite set of electron-hole pair states,

$$\psi_{\nu}(z_e, z_h, \rho) = \sum_{n=1}^{N} \Phi_n(z_e, z_h) \phi_n(\rho),$$

and

$$\Phi_n(z_a, z_b) = \varphi_a^i(z_a)\varphi_b^j(z_b), \quad n = (i, j)$$

where  $E_{_{\boldsymbol{\sigma}}}$  is the bandgap of the well material.

The electron and hole wave functions in the growth direction  $\varphi_e^i(z_e), \varphi_h^j(z_h)$  are calculated by solving the Schrodinger equation in real space. The exciton wave functions in the in-plane motion  $\phi_e(\rho)$  are calculated using the finite difference scheme in the matrix form.

When the quantum confined structure is embedded in the cavity, an exciton in such a structure can interact with a photon inside the cavity and forms an exciton-photon quasiparticle called a polariton. The exciton-photon interaction is treated by solving coupled material and Maxwell's equation.

$$\left(-\frac{\hbar^{2}}{2m}\nabla_{R_{xy}}^{2} + H_{ex} + E_{g} - \hbar\omega - i\gamma\right)Y(r,R) = M(r)E(R)$$

$$\nabla \times H = \frac{1}{c}\frac{\partial D}{\partial t}, \qquad \nabla \times E = -\frac{1}{c}\frac{\partial B}{\partial t}$$

$$\nabla \cdot B = 0, \qquad \nabla \cdot D = 0$$

where r is the relative coordinate, R is the center of mass coordinate,  $H_{ex}$  is the exciton Hamiltonian,  $\gamma$  is the phenomenological damping, E(R) is the electric field, Y(r,R) is the microscopic polarization and M(r) is the microscopic dipole moment. The magnetic field is  $B = \mu H$  and the electric displacement field is  $D = \varepsilon E$ , where  $\mu$  is the permeability and  $\varepsilon$  is the permittivity of a medium.

To study the dipolaritons, we estimate the fraction of direct exciton (DX), indirect exciton (IX), and cavity mode (CM) in each of them by evaluating the polariton brightness ( $\mathbb{F}$ ) and the dipole moment (D) which we define as

$$\mathbb{F} = \mathbb{N}^{-1} \left| \int \mathbf{P}(z_e, z_h, \rho) dz \right|^2$$

$$\mathbf{D} = \mathbb{N}^{-1} \iiint \left| \mathbf{P}(z_e, z_h, \rho) \right|^2 (z_e - z_h) d\rho dz_e dz_h$$

$$\mathbb{N} = \iiint \left| \mathbf{P}(z_e, z_h, \rho) \right|^2 d\rho dz_e dz_h$$

where  $\mathbb N$  is a normalization integral.

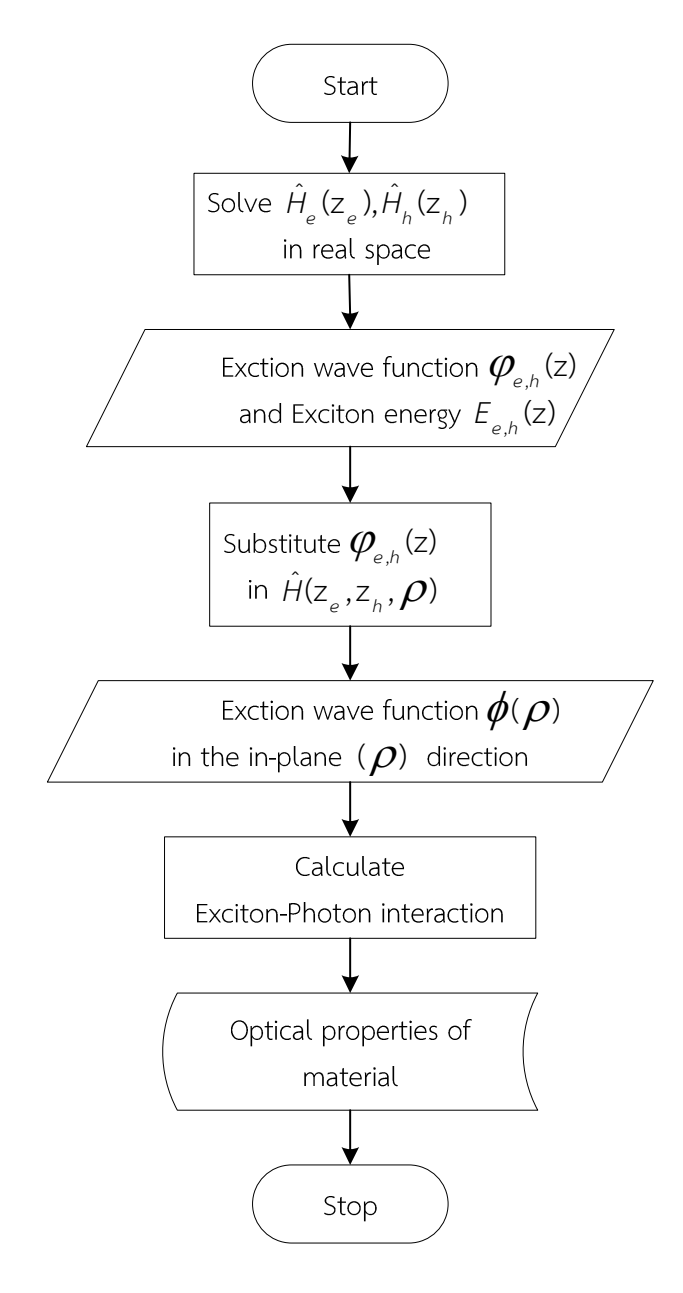


Fig. 3: Flowchart of the program.

The  $P(z_e, z_h, \rho)$  is the microscopic excitonic polarization which can be expand into the complete set of exciton eigenfunctions;

$$P(z_e, z_h, \rho) = |d_{cv}|^2 \sum_{v} \frac{\psi_v(z_e, z_h, \rho) X_v(\omega, k)}{E_v + \hbar^2 k^2 / 2M - \hbar\omega - i\gamma}$$

The expansion coefficients are then given by

$$X_{\nu}(\omega,k) = \int E(\omega,k;z) \psi_{\nu}(z_{e},z_{h},0) dz$$

The relationship between the DX, IX, and CM components ( $C_{DX}$ ,  $C_{IX}$ ,  $C_{CM}$  respectively) is then given by

$$\left(\frac{C_{_{IX}}}{C_{_{X}}}\right)^{2} \approx \alpha D$$
 and  $\left(\frac{C_{_{CM}}}{C_{_{X}}}\right)^{2} \approx \beta \mathbb{F}$  and  $C_{_{X}}^{2} = C_{_{DX}}^{2} + C_{_{IX}}^{2}$ 

Indeed, the content of the IX is determined by the dipole moment, the brightness F is proportional to the exciton oscillator strength and therefore to the exciton-CM coupling. Normalized fractions  $C_{DX}$ ,  $C_{DX}$ ,  $C_{CM}$  are then calculated by taking the values of F, D, and N at the polariton frequencies.

#### 5. Results and Discussion

In this work, we consider Al<sub>x</sub>Ga<sub>1-x</sub>As/GaAs (with x=0.33) and Ga<sub>1-x</sub>In<sub>x</sub>N<sub>y</sub>As<sub>1-y</sub>/GaAs (with x=0.35, y=0.005) quantum well (QW) structures in order to study the effect of structural parameters on electron and hole energies. A QW layer has narrow band gap, while a wider band gap material is used as a surrounded barrier. The step layer or tilted layer can be added to the structure to form the step QW and tilted QW structure. The additional layer is the same material as the surrounded layer but has different x and y contents and their parameters are calculated by linear interpolation between the well layer and barrier layer. The parameters for electron/hole mass and potential are shown in Table. 1.

Table 1: Parameters used in the calculation.

Parameter (unit)	Al <sub>x</sub> Ga <sub>1-x</sub> As/GaAs	Ga <sub>1-x</sub> In <sub>x</sub> N <sub>y</sub> As <sub>1-y</sub> /GaAs
V <sub>e</sub> (meV)	267.48	438.83
V <sub>h</sub> (meV)	144.03	109.70
Well layer	GaAs	GalnNAs
m <sub>1,e</sub> (m <sub>0</sub> )	0.0665	0.0656
m <sub>1,h</sub> (m <sub>0</sub> )	0.34	0.3447
Barrier layer	AlGaAs	GaAs
m <sub>2,e</sub> (m <sub>0</sub> )	0.0941	0.0665
m <sub>2,h</sub> (m <sub>0</sub> )	0.476	0.34

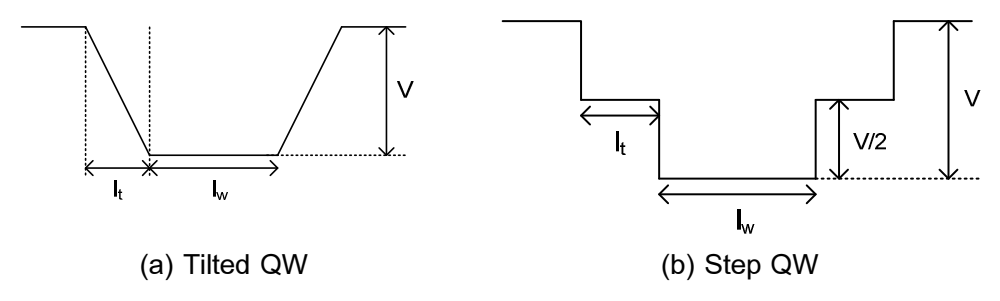
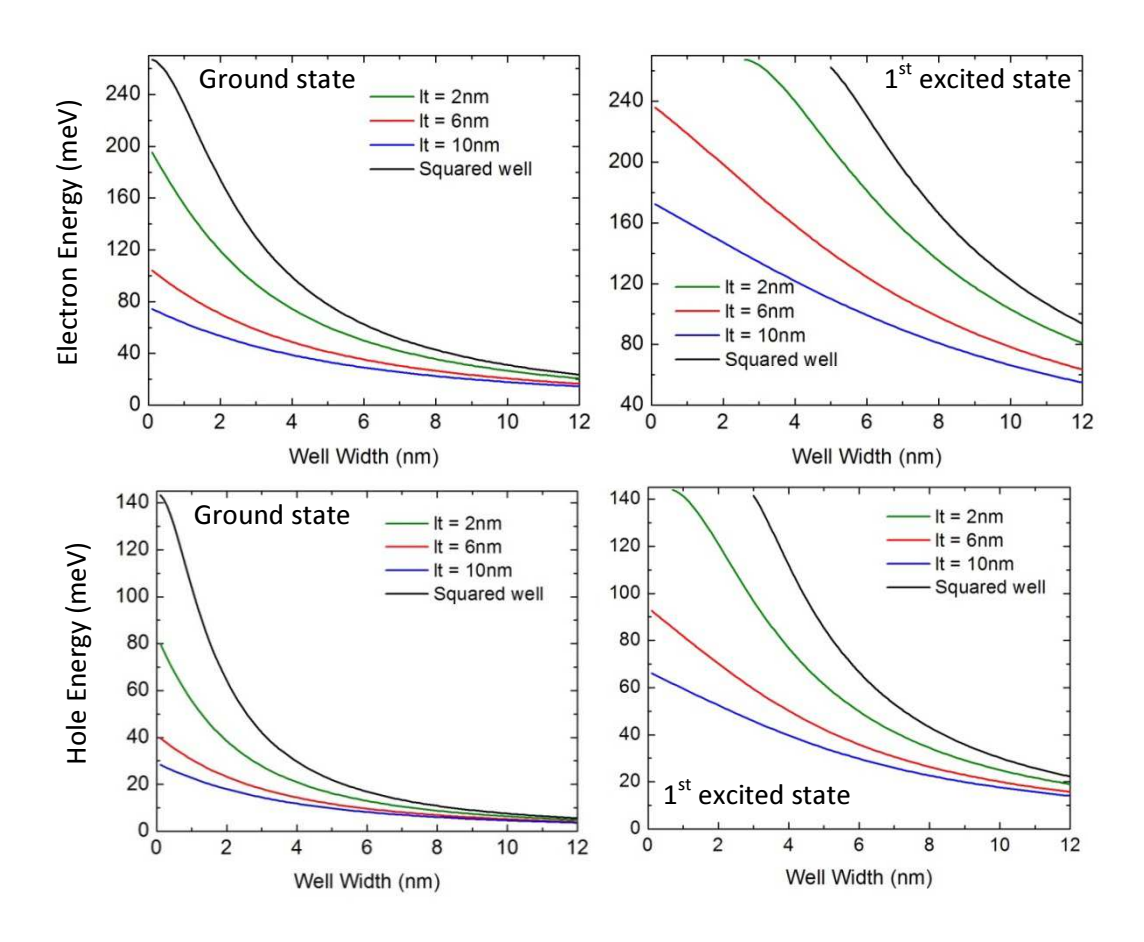


Fig. 4: The tilted and step quantum well structures.

## Electron and Hole energies in tilted Quantum Well

We consider the GaAs/AlGaAs and GaInNAs/GaAs tilted single quantum well (SQW) in order to study the effect of tilted layer on the electron and hole energies. The tilted SQW profile is shown in Fig. 4(a). The tilted layer width ( $L_t$ ) and well width ( $L_w$ ) are varied from 0.1 nm to 2 nm. The results show that the electron and hole energies decrease with increasing the well width and tilted layer width.



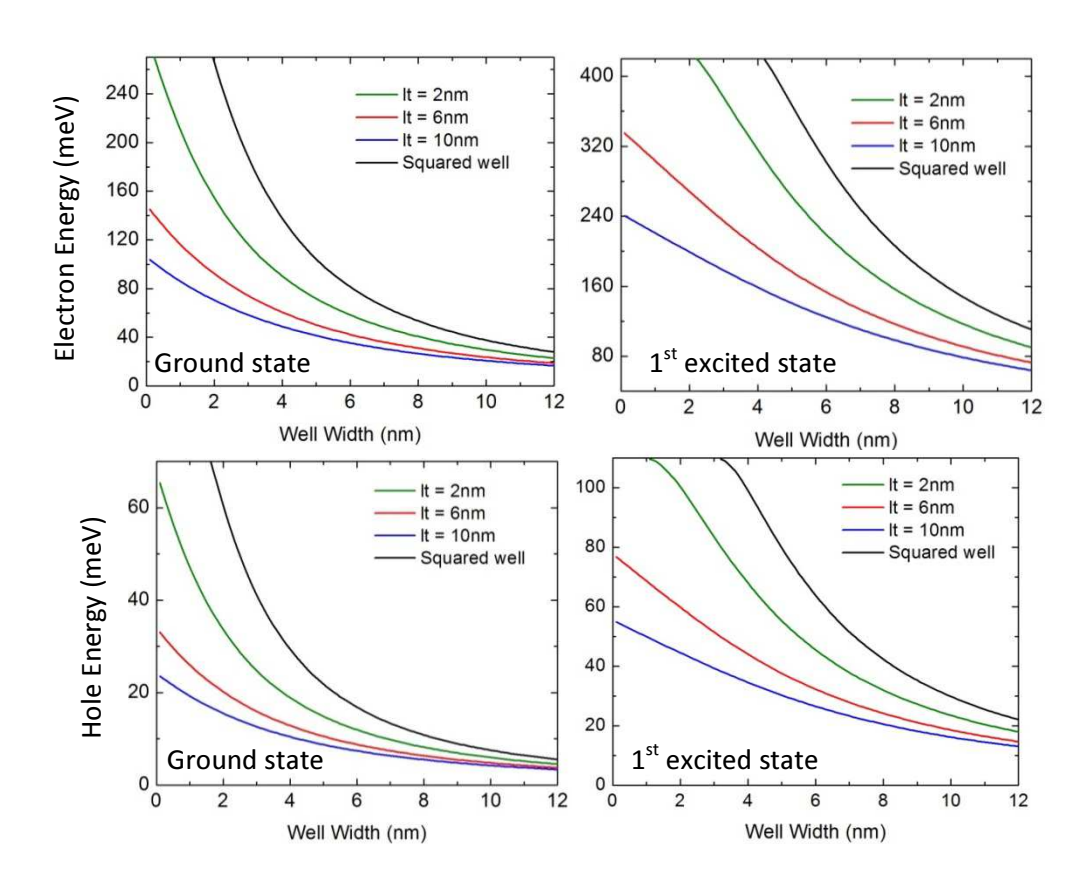


Figure 5 and Figure 6 demonstrate the ground state (GS) and the first excited state (<sup>1st</sup>ES) energies for both electron and hole. It is found that the trends are similar for both structures, but the values are different due to the difference of the potential height (see table 1). For example, the potential height for electron in GaAs/AlGaAs is 267.48 meV, while that in GalnNAs/GaAs is 438.83 meV which is nearly two times larger than the case of GaAs/AlGaAs. Therefore, we can use all these results to study the effect of potential height on the electron and hole energies as well. The electron energies in both structures are shown in Fig. 7 for fixed well width and tilted layer width. For fixed well width, the electron energies in both structures decrease with the same trend and the energy difference between the two structures are nearly constant. In contrast, if we fix the tilted layer width and vary the well width the electron energy in larger potential height (GalnNAs/GaAs) will decrease more rapidly than the smaller height (GaAs/AlGaAs).

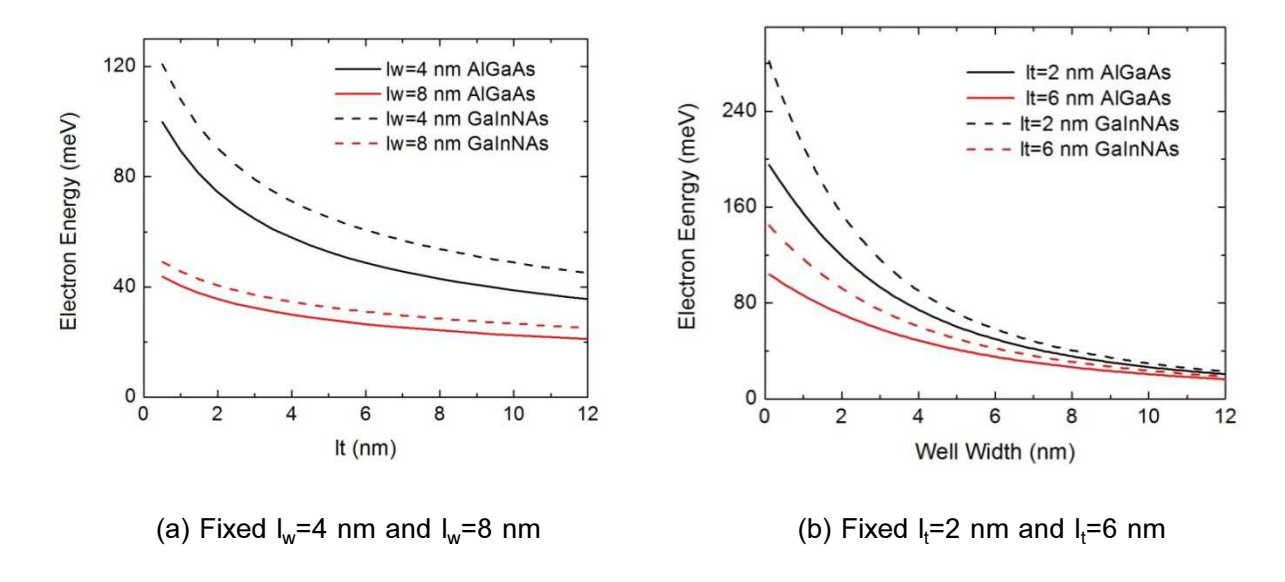


Fig. 7: Electron energies in GaAs/AlGaAs and GaInNAs/GaAs tilted quantum well structures.

## Electron and Hole energies in Step Quantum Well

The electron and hole energies in GaAs/AlGaAs step QW structure [Fig. 4(b)] with different step layer widths are calculated as a function of well width (Fig. 8). The energies for all cases decrease with increasing the well width. Adding the step layer gives rise to the decrease of electron and hole energies compared to the single squared well structure. For the ground state (GS), the energy of electron (hole) rapidly drops from 265 meV (142 meV) in single squared well to 200 meV (90 meV) in the case of 2-nm step layer. However, the energy changes very small when the step layer is increased from 6-nm to 10-nm.

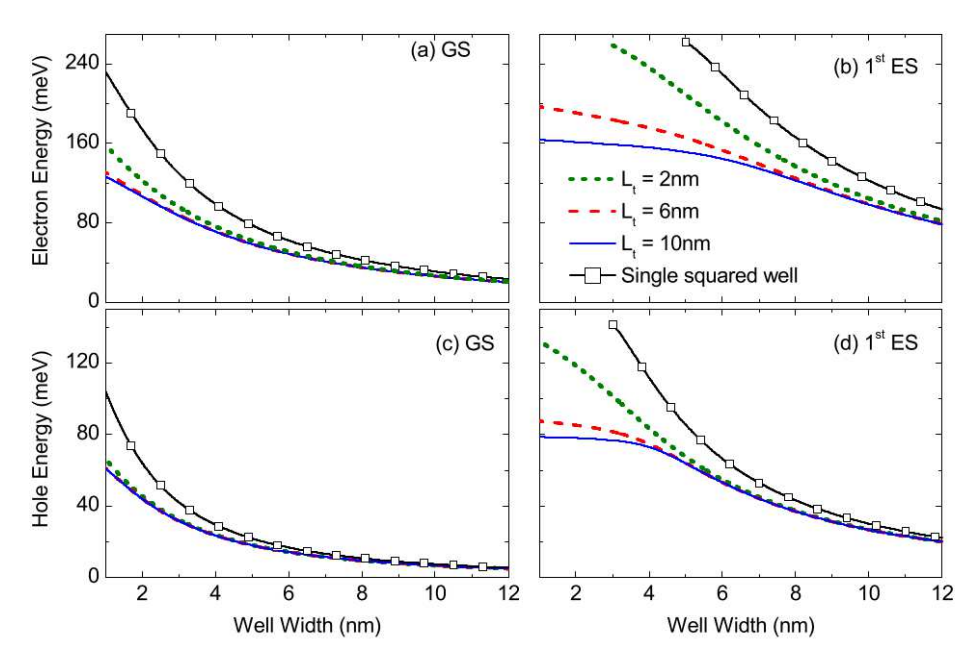


Fig. 8: Electron and hole energies in GaAs/AlGaAs step QW structure as a function of well width for  $L_t=2$  nm (solid), 6 nm (dashed) and 10 nm (dotted).

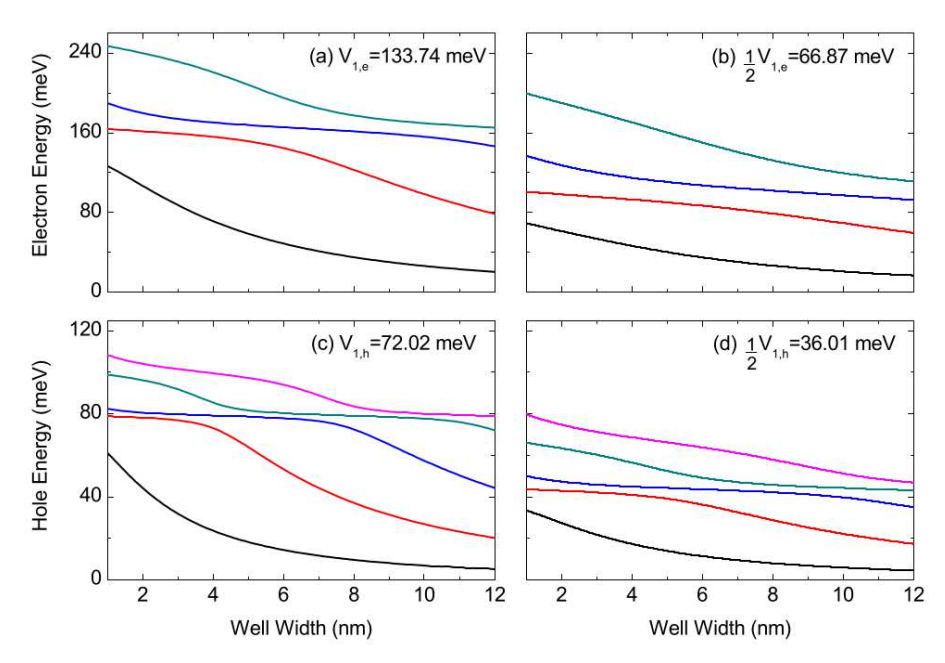


Fig. 9: Four states of electron and five states of hole in GaAs/AlGaAs step QW structure for  $L_t$  =10 nm and different step potential as a function of well width for different potentials.

It is clearly seen from Fig. 8(a) and Fig. 8(c) that the electron and hole energies in 10-nm step QW are very close to that of 6-nm step layer case. Only a small difference is observed at a narrow well width. The reason is that all these energies are lower than the step potential  $(V_{1,e}=133.74 \text{ meV})$  for electron and  $V_{1,h}=72.02 \text{ meV}$  for hole) residing in the lower QW, so that the change of step layer width does not affect to these energy levels. At approximately  $L_w=6 \text{ nm}$  ( $L_w=2 \text{ nm}$ ), the electron (hole) energies in step QW for all cases are the same at the energy of around 60 meV (40 meV). It is observed at a narrower well in the case of hole because of the heavier mass and lower potential of hole. For the first excited state ( $^{1st}ES$ ) [Fig. 8(b), 8(d)], it is also observed a large difference in energy between 2-nm and 6-nm cases and only a small change between 6-nm and 10-nm of step layer. Again, when the energies are lower than the potential  $V_1$  the state already occupies in the lower well. The step layer has no longer influence on the energy and all levels tend to the same level.

Figure 9 shows the electron and hole energies in a 10-nm step QW structure (four states of electron and five states of hole). It is notices that there are excited states lie parallel at the energy of approximately 160 meV for electron and 80 meV for hole which are near the bottom of the step potential. The hole energy in Fig. 9(c) shows that the first excited state energy remains unchanged at 80 meV at  $L_w$ =1 nm, while the second excited state starts at around 95 meV and decreases to 80 meV. The second excited state then remains at this level and parallel to the first excited state for  $L_w$ <4. When  $L_w$ >4 nm the first excited state drops down to lower energy, the third excited state comes to the level of 80 meV and is parallel to the second excited state for the well width of  $L_w$ =5-8 meV. The same also happens for the fourth excited state and so on. The energy splitting of two

paralleling states is about 10 meV for electron and 3 meV for hole. The step potential  $V_1$  is decreased by a factor of two in order to see how the electron and hole energies change [fig. 9(b), 9(d)]. It is found that the energy trend does not change, the calculated energies only shift down to lower energy due to a lower potential. There also be two paralleling energy levels at the energy which is above the step potential  $V_1/2$ . The splitting between the two energies is twice compared to the case of  $V_1$  step potential. The hole wave functions of five states in GaAs/AlGaAs step QW structure are demonstrated in Fig. 10. The white dashed lines indicate the region inside the lower well, while the while dotted lines show the edge of the step layer. It is found that there are two broadening peaks in the step well region when the excited state remains at the parallel level ( $L_w$ <4 nm for  $^{1st}ES$ ,  $L_w$ <8 nm for  $^{2nd}ES$ ,  $4 < L_w$ <11 nm for  $^{3rd}ES$  and  $L_w$ >8 nm for  $^{4th}ES$ ). As we know, the  $N^{th}ES$  excited state should has N maxima of the wave function. However, all peaks in the middle always very small compared to the two broadening peaks. The sharp peaks inside the well region in Fig. 10(b) for  $L_w$ >4 nm and in Fig. 10(c) for  $L_w$ >8 nm are observed when hole energy drops down to the level below the step potential, corresponding to a strongly decrease of energy as the well width increases in Fig. 9.

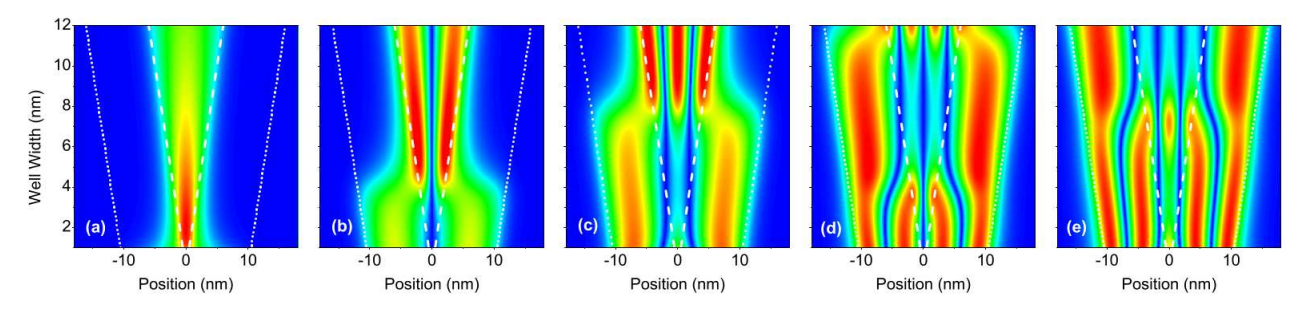


Fig. 10: Wave functions of five hole state in GaAs/AlGaAs step QW structure with  $L_t$  =10 nm for (a) GS, (b)  $^{1st}$ ES, (c)  $^{2nd}$ ES, (d)  $^{3rd}$ ES, and (e)  $^{4th}$ ES states. The region inside two white dashed lines is the lower well region, while two white dotted lines indicate the step layer edges.

We have also calculated the electron and hole energies in the GalnNAs step QW structure (Fig. 11). The parameters used in the calculation are shown in Table. 1. The results show that the well width dependence of energies looks very similar to those in GaAs/AlGaAs step QW structure. The electron and hole energies are calculated for the electric field up to 200 kV/cm and the step layer width is fixed at L<sub>t</sub>=10 nm. The results show that the ground state energy remains nearly constant at low electric field and the energies then linearly decrease with increasing field giving rise to an anticrossing in energy (Fig. 12). This anticrossing happens at larger field for wider well width. The first four energy states of electron and hole for L<sub>t</sub>=8 nm are demonstrated in Fig. 12(c)-(d). The anticrossing of GS-<sup>1st</sup>ES energy happens at around F=130 kV/cm for electron and F=75 kV/cm for hole. The electron wave functions at F=120 kV/cm (before the electron anticrossing) and F=140

kV/cm (after the electron anticrossing) in Fig. 12(e) show that the maximum of the wave function changes from the well layer to step layer. The reason why electron is now confined in the step layer after the anticrossing is because the large field makes the step layer potential becomes lower than the well potential. Moreover, the tilted potential due to the electric field can cause the tunneling of electron/hole through the surrounded barrier which can be observed the oscillation in the left region as shown in Fig. 12(e). A larger field leads to a larger tunneling effect.

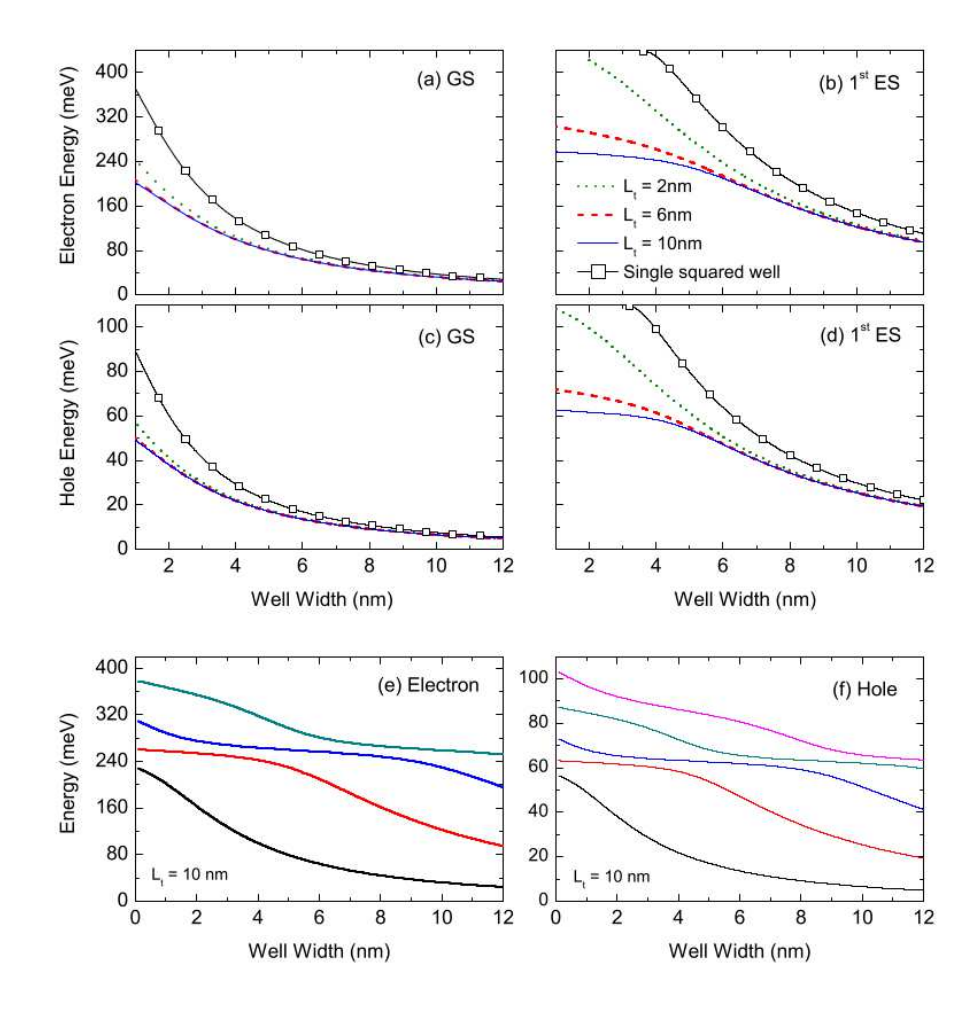


Fig. 11: Electron and hole energies in GalnNAs/GaAs step QW structure as a function of well width for  $L_t$ =2 nm (solid), 6 nm (dashed) and 10 nm (dotted). The four electron states and five hole states for  $L_t$ =10 nm are shown in (e) and (f) respectively.

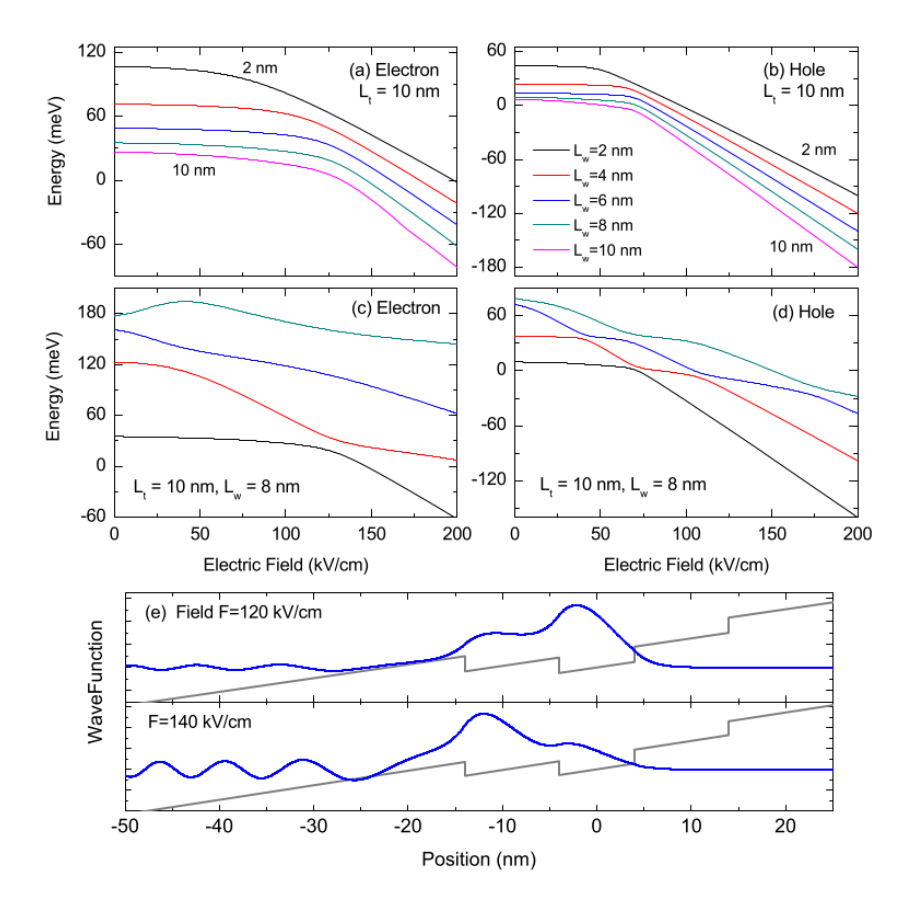


Fig. 12: Electric field dependence of electron and hole energy in GaAs/AlGaAs step QW structure.

The ground state electron wave function at F=120 kV/cm and F=140 kV/cm are demonstrated in (e).

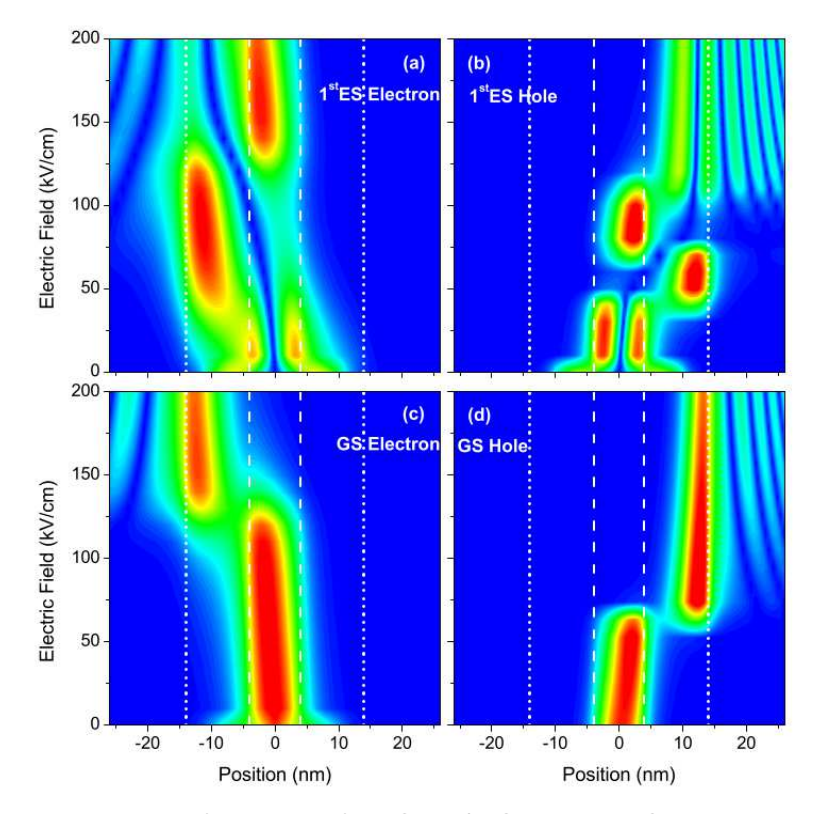


Fig. 13: Electron and hole wave functions of in GaAs/AlGaAs step QW structure for  $L_t$ =10 nm and  $L_w$ =8 nm. The dotted lines indicate the step layer edges.

The electron and hole wave functions for  $L_t$ =10 nm and  $L_w$ =8 nm are plotted as a function of electric field (Fig. 13). Electron and hole ground states are not confined at the center anymore. Electron moves to the left and hole moves to the right due to the electric field. The wave function maxima of electron (hole) are observed at the left (right) wall. The change of wave function localization occurs at the energy anticrossing. After the anticrossing, the ground state electron locates in the left step layer, while the first excited state electron is confined in the well layer instead. The same situation also happens in the case of hole, but hole will move to the right. Note that ground state electron is in the left step layer and ground state hole resides in the right step layer at large field, so that it is possible to form an indirect exciton in the step QW structure.

## Exciton states in Coupled Quantum Well (CQW)

We consider the GalnNAs/GaAs CQW structure consisting of GaAs layer sandwiched between GalnNAs layers. The GaAs barrier width is fixed to 5 nm, while the GalnNAs well width is varied from 5 nm to 10 nm. The electric field (F) up to 60 kV/cm is applied in the growth direction. Due to the tunneling through the barrier, the singlet state splits into doublet states. Their energy levels exhibit the Stark effect when the electric field is applied; one state is red shift, while the other is blue shift. Consequently, the energy splitting of doublet state increases with increasing the electric field. The electric field breaks the symmetry of the wave function and makes the wave functions of the doublet states occupies in different QW.

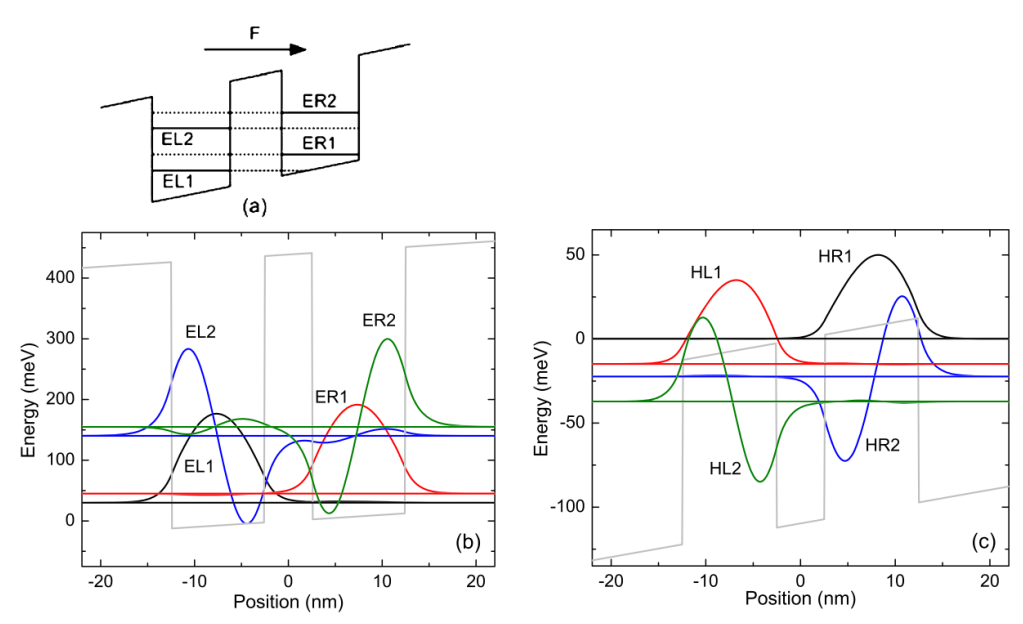


Fig. 14: Electron and hole wave functions for 10-5-10-nm GalnNAs/GaAs CQWs at F=10 kV/cm. We denote the four states as EL1, ER1, EL2, ER2 (HL1, HR1, HL2, HR2) indicating the localization of electron (hole) in a left (L) or right (R) QW.

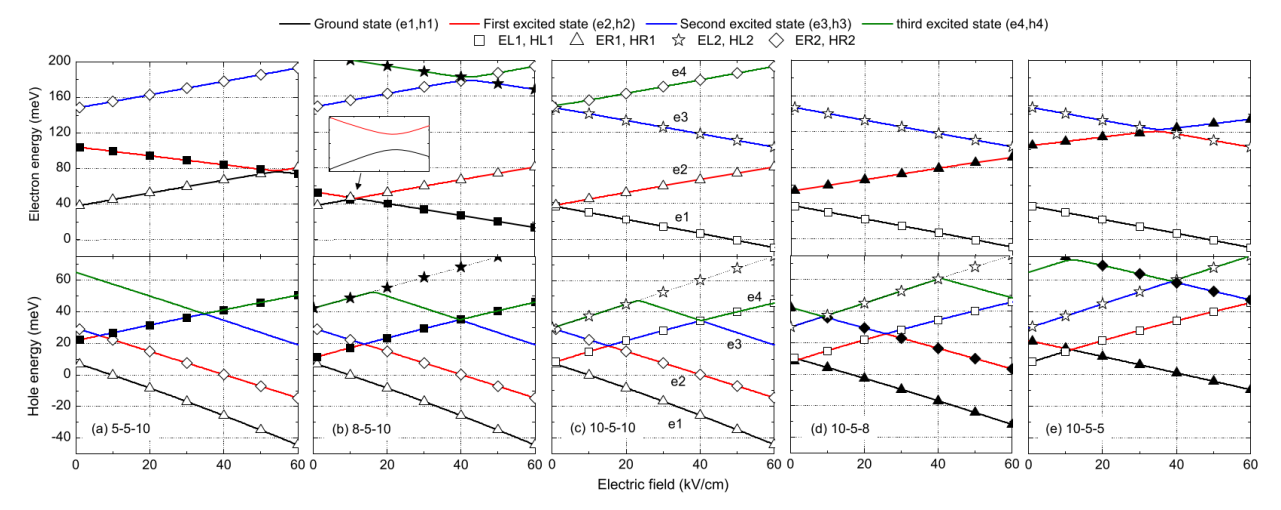


Fig. 15: Electron and hole energy as a function of electric field for (a) 5-5-10-nm, (b) 8-5-10-nm, (c) 10-5-10-nm, (d) 10-5-8-nm and (e) 10-5-5-nm GaInNAs/GaAs CQWs. The closed symbols show the energy of doublet states which is shift due to the change of well width, while the opened symbols denote the unchanged states.

Figure 14 shows the wave function of electron and hole for symmetric QW structure (10-5-10-nm) at F=10 kV/cm. It is clearly seen that the electric field makes the maxima of wave functions locates in one well only; e1, e3 and h2 in the left well and e2, h1 and h3 in the right well. The field dependent energy levels of electron and hole are demonstrated in Fig. 15. We denote the electron and hole states occupying in the left QW (namely EL and HL) by square and star symbols, while electron and hole states locating in the right QW (namely ER and HR) are represented by triangle and diamond symbols [see Fig. 15(a)]. Under the applied electric field, EL(HR) states exhibit the red Stark shift and ER(HL) is blue Stark shift. This Stark effect is enhanced when the electric field increases and gives rise to a larger energy splitting of the doublet. This can make the EL-ER or HL-HR crossing at some value of electric field, for example the HR1-HL2 crossing at F=15.2 kV/cm in the hole energy of 10-5-10-nm CQWs [Fig. 15(c)]. The electron and hole energies are also calculated in the case of asymmetric QW structures. It is found in Fig. 15(a)-15(b) that the decrease of the left QW width results in the increasing of EL1, EL2, HL1 and HL2 energies but ER1, ER2, HR1 and HR2 are the same position as in the case of 10-5-10-nm structure. This is because EL1, EL2, HL1 and HL2 are all the states occupying in the left well, so the decrease of the left width will affect all these states. In addition, the shift of energy level gives rise to the anticrossing of the electron and hole energy at different electric field for different well width. For 5-5-10-nm CQWs, the energy of EL1 state is higher than that of ER1 level. As a result, the ground state electron (e1) in this case will occupy in the right QW and exhibit the blue shift, while the first excited state electron (e2) is confined in the left QW with the red shift effect. The same situation also happens when the

right QW is decreased. The ER1, ER2, HR1 and HR2 levels are shifted to higher energy, while the EL1, EL2, HL1 and HL2 are still the same energy as shown in Fig. 15(d)-15(e).

We have also calculated the exciton states and their optical properties for the electric field up to 60 kV/cm. The exciton states is expanded into the set of e-h pair states including 2 electron (e1,e2) and 3 hole (h1,h2,h3) states. The exciton state for 10-5-10-nm CQWs are demonstrated in Fig. 16. The area of each circle is proportional to the oscillator strength of each exciton state. It is found that there are two bright (direct) exciton states with large oscillator strengths, namely DX1 and DX2, at the energy of 38 meV. These two states are overlap to each other which clearly seen in the inset of the figure. The DX1 state is dominated by an electron and a hole in the left QW which is EL1 and HL1 levels. The red shift of EL1 energy is compensated by the blue shift of HL1 energy, so that the DX1 energy changes only 7-8 meV in this range of the electric field. The DX2 state is formed from an electron and a hole in the right QW (ER1 and HR1). Again, the compensation of ER1 (blue shift) and HR1 (red shift) leads to a small change of DX2 exciton energy. The exciton energies for asymmetric 10-5-8-nm and 5-5-10-nm structures are also shown in Fig. 17. For 10-5-8nm CQWs, the DX1 energy remains unchange because the EL1 and HL1 are the same position as in the case of 10-5-10-nm CQWs, while the DX2 energy increases to higher energy due to the increase of ER1 and HR1 energy levels. In Fig. 17(b), there is only DX2 states locates at the same energy position because the ER1 and HR1 energy levels are still the same position compared to 10-5-10-nm CQWs. On the other hand, the DX1 is absent from this range of energy but it will appear at higher exciton energy due to the EL1 and HL1 energy levels increase compared to the these levels in 10-5-10-nm structure as seen in Fig. 15(a)-15(b).

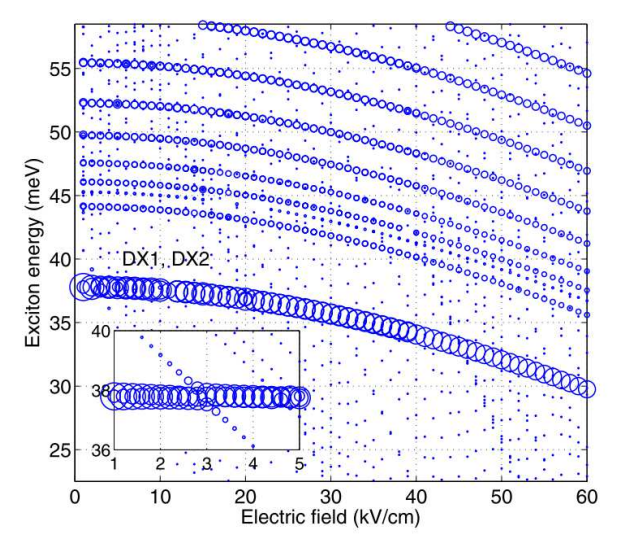


Fig. 16: Exciton energy as a function of electric field for 10-5-10-nm GalnNAs/GaAs CQWs. The circle area of each state is proportional to its oscillator strength. The inset shows the direct-indirect crossover of the exciton ground state.

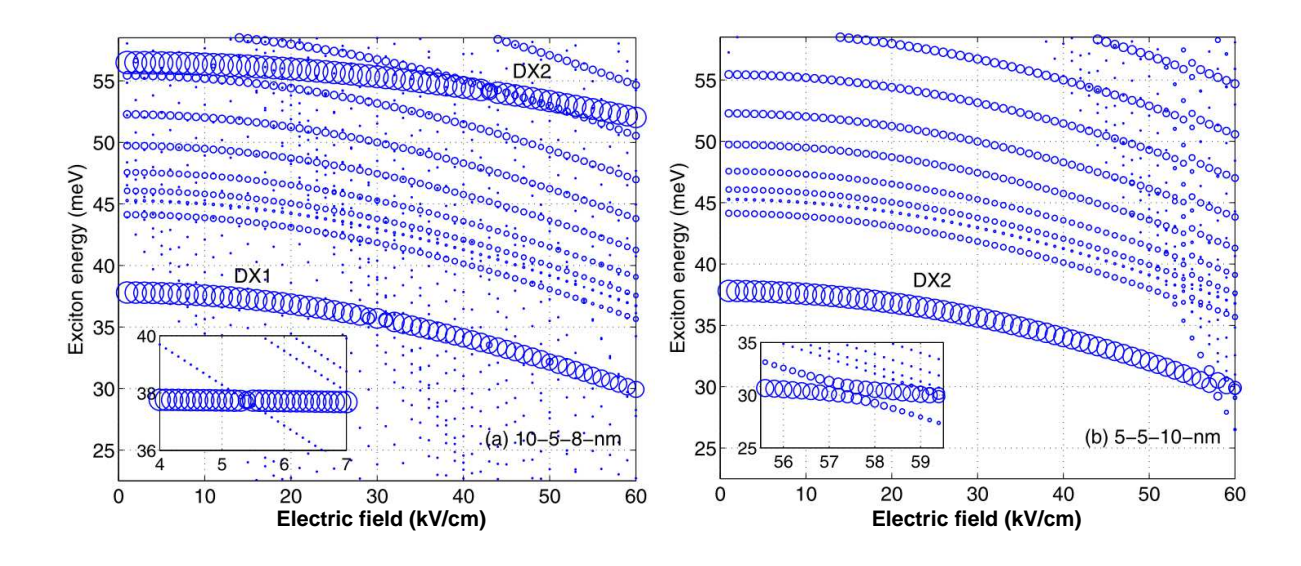


Fig. 17: Exciton energies as a function of electric field for (a) 10-5-8-nm and (b) 5-5-10-nm GalnNAs/GaAs CQWs.

## Polariton states in Quantum Well Microcavity

A typical semiconductor microcavity consists of a cavity layer sandwiched between two distributed Bragg reflectors (DBRs) as shown in Fig. 18. A DBR is usually made of alternating  $\lambda/4$  layers of different semiconductor materials, with high and low refractive indices. The incident light is reflected at the DBR interface and only a single wavelength, namely that as a cavity mode, is transmitted (indicated as a sharp peak in the reflectivity spectra). This creates also a stop-band in the transmission spectrum. Hence, the DBR behaves as a high reflective mirror for wavelengths within the stop-band. When the quantum confined structure is embedded in the cavity, an exciton in such a structure can interact with a photon inside the cavity and forms an exciton-photon quasiparticle called a polariton. An exciton mode coupled to one photon gives rise to two polariton modes (double peaks are seen in the reflectivity spectra). The lower energy mode is called lower polariton (LP) branch, while the upper polariton (UP) branch refers to the mode with higher energy. In the strong coupling regime, the photon is bounced back and forth between the two DBR mirrors and is absorbed by an exciton.

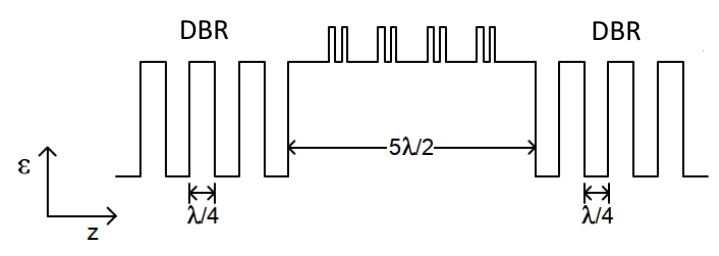


Fig. 18: Schematic of a microcavity-embedded GalnNAs quantum well structure.

We concentrate on a microcavity structure which consists of four GalnNAs DQWs of 8-5-10nm placed at the antinodes of the electromagnetic field inside a  $5\lambda/2$  cavity sandwiched between 17 and 21 pairs of GalnNAs/GaAs distributed Bragg reflectors (DBRs). The exciton energies as a function of electric field for 8-5-10-nm DQWs are shown in Fig. 19. In order to study the excitonphoton strong coupling, the cavity mode is fixed at 1.411 meV and 1.427 meV near the DX states (DX2 at lower energy and DX1 at higher energy). The results are demonstrated in Fig. 20. Basically, the DX strongly couples to the cavity mode and creates a polariton. The IX itself does not form a polariton, as it has much smaller oscillator strength. Note that the IX component in each polariton state is very small compared to DX and CM contributions, except at approximately F=12 kV/cm where the DX-IX crossover is observed--the IX fraction is maximum. Although the indirect exciton does not directly couple to the cavity mode, it is electronically coupled to the direct exciton. Therefore, it can be say that the indirect exciton is coupled to the cavity mode via the direct exciton. A resulting mixed state of such a three-level system is a dipolariton state that acquires a large electric dipole moment form indirect exciton. The dipolariton is observed at around F=12 kV/cm in state 1 for the case of cavity mode at 1.411 eV [Fig. 20(a)]. The CM and IX fractions are around 0.4 and DX component is 0.2.

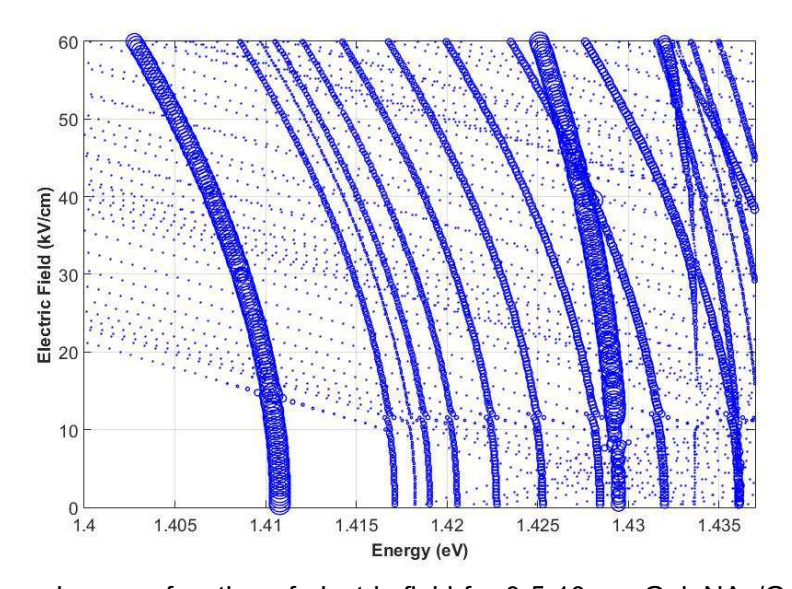


Fig. 19: Exciton energies as a function of electric field for 8-5-10-nm GalnNAs/GaAs CQWs.

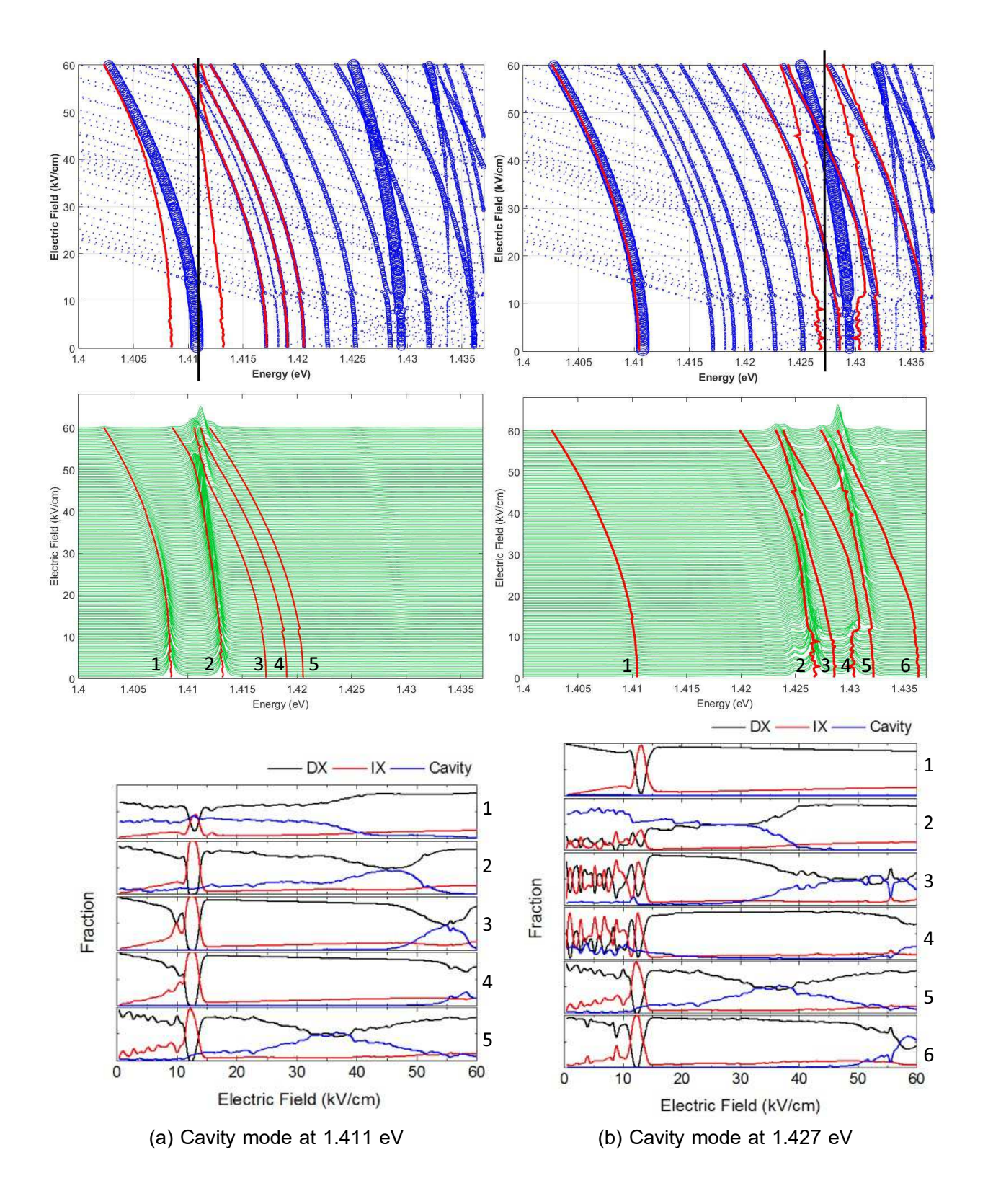


Fig. 20: DX, IX and CM fractions for polariton states.

#### 6. Conclusion

In this work, the electron and hole energies and wave functions in the QW structures have been theoretically studied by solving straight forward the Schrodinger equation in real space. The effects of width and potential profile on their energies are investigated. We consider several potential shape of the GaAs/AlGaAs and GalnNAs/GaAs QWs including step QW, tilted QW and squared QW structures. The width of additional layer (step layer/ tilted layer) inserting to the squared QW results in the decrease of electron and hole energies, the wider the lower.

When the electric field is applied to the growth direction, the symmetry of the wave function is broken and the electron and hole move in opposite direction. As a result, the indirect exciton can be formed in the double QW structure. In the calculation, the exciton states are calculated from the obtained electron and hole states. The oscillator strength of exciton is calculated as a function of applied electric field. The results show the decrease of the oscillator strength of the ground state exciton, corresponding to the switching from direct to indirect states. The anticrossing in exciton ground state happens at approximately F=12 kV/cm for GalnNAs/GaAs CQWs structure. In this structure, it is also found the two direct exciton states namely DX1 and DX2 which has large oscillator strength. For symmetric 10-5-10-nm structure, the DX1 and DX2 states have the same eneries. However, one of them is shifted to higher energies if one of well width is reduced forming the asymmetric structure.

In the polariton calculation, the GalnNAs/GaAs CQWs are placed in the microcavity in order to study the exciton and photon interaction. The DX strongly couples to the cavity mode and creates a polariton which has large oscillator strength but small dipole moment. The IX has small oscillator strength, so that it does not form a polariton. However, it is electronically coupled to the direct exciton via the tunneling across the barrier. Therefore, the polariton state with a mix of DX, IX and cavity mode can be formed and so called the dipolariton state. The dipolariton will acquire a large oscillator strength from DX and a large dipole moment from indirect exciton. In this work, the dipolariton state is observed when the cavity mode strongly couples to the ground state exciton at the anticrossing (F=12 kV/cm). The IX and cavity mode fractions are around 0.4 and DX component is about 0.2. In addition, the strong coupling can be controlled by electric field.

## 7. Output (Acknowledge the Thailand Research Fund)

### 7.1 International Journal Publication

- 1) W. Bukaew and <u>K. Sivalertporn</u>, "Study on electron and hole states in tilted quantum well structures" Journal of Physics: Conference Series 1380, p012079 (2019).
- 2) N. Rueangnetr and <u>K. Sivalertporn</u>, "Effect of quantum well width on the electron and hole states in different single quantum well structures" Journal of Physics: Conference Series 1380, p012082 (2019).
- 3) P. Poopanya, N. Rueangnetr, W. Bukaew, and <u>K. Sivalertporn</u>, "Effect of step layer width and electric field on single-particle states in step quantum well structures (in process, submitted to International Journal of Nanoscience; I will inform later when the paper has been published)
- 4) P. Poopanya and <u>K. Sivalertporn</u>, "Exciton-Photon strong coupling regime and Dipolariton states in GalnNAs/GaAs quantum well microcavity" (in process; I will inform later when the paper has been published)
  - 7.2 Application -
  - 7.3 Others: Attend the international conference on the Siam Physics Congress 2019 (SPC2019).

## 8. Appendix

## 1) Publication in the international journal:

Siam Physics Congress 2019 (SPC2019): Physics beyond disruption society

**IOP Publishing** 

Journal of Physics: Conference Series

**1380** (2019) 012079 doi:10.1088/1742-6596/1380/1/012079

## Study on electron and hole states in tilted quantum well structures

#### W Bukaew and K Sivalertporn\*

Department of Physics, Faculty of Science, Ubonratchathani University, Ubon Ratchathani, 34190, Thailand

\*E-mail address: kanchana.s@ubu.ac.th

Abstract. In this study, the energy states of electron and hole in Ga<sub>x</sub>In<sub>1-x</sub>N<sub>y</sub>As<sub>1-y</sub>/GaAs tilted quantum well structure have been theoretically investigated. The content of x and y are 0.65 and 0.005 respectively. The energy states and wave functions have been calculated by solving the Schrödinger equation in real space. The well width of 2-10 nm, barrier width of 2-10 nm and tilted layer width of 1-3 nm are considered in this work. The results show that the electron and hole energies decrease with increasing the well width and tilted layer width. The wave functions are both symmetric (ground state) and anti-symmetric (the first excited state), and spread out as the well width increases. In addition, the barrier width of couple tilted quantum well structure has also been studied. It is found that the probability of finding electron and hole are equal in both wells and the wave function within barrier layer decreases with increasing the barrier width as well. The ground state energy increases and the first excited state energy decreases as the barrier increases. As a result, the two states tend to the same level when the barrier is more than 8 nm. This is because the wide barrier can decrease the interaction between two quantum wells and makes each quantum well acts as an isolated quantum well with no interaction between them.

#### 1. Introduction

In past decades, the semiconductor quantum well (QW) have been experimentally and theoretically studied due to their potential applications in optoelectronic devices [1-3]. A typical structure is a single QW (SQW) consisting of one well layer sandwiched between two barrier layers. The electron and hole are confined in QW layer and can create an electron-hole pair called a direct exciton. However, the direct exciton has very short lifetime. Therefore, the couple QWs (CQWs) – two wells separated by a thin barrier – have been attracted much attention since the indirect exciton with long lifetime can be created in such a structure [4]. To study the optical property, the exciton energy, binding energy and oscillator strength have been investigated for different parameter [5-8]. In addition, there are a number of research works concentrate on the electron and hole states only (not the exciton state). However, it is also very important since these states are used to calculate the exciton state and properties in the next step. The effects of structural parameters including well width, barrier width or potential profile on the single-particle energies and wave functions have been theoretically investigated [9-10].

In this work, the GaInNAs/GaAs tilted quantum well (TQW) structures are considered in order to study the effect of tilted layer on the electron and hole energies. The energy levels and wave function in single and coupled TQWs are calculated for different parameters.

Content from this work may be used under the terms of the Creative Commons Attribution 3.0 licence. Any further distribution of this work must maintain attribution to the author(s) and the title of the work, journal citation and DOI.

Published under licence by IOP Publishing Ltd

**1380** (2019) 012079 doi:10.1088/1742-6596/1380/1/012079

#### 2. Theoretical model

Let us consider symmetric single tilted quantum well (STQW) and coupled tilted quantum well (CTQW) consisting of a well layer sandwiched between two tilted layers as shown in figure 1.

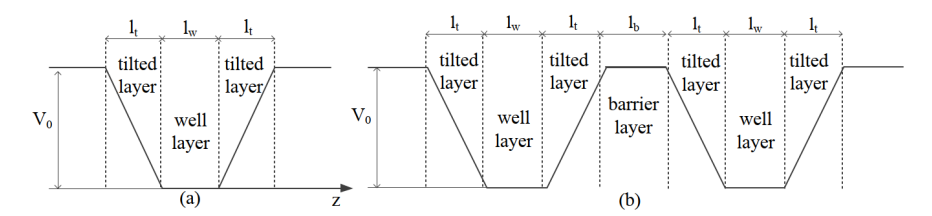


Figure 1. Schematic structures for (a) STQW and (b) CTQW.

Under the effective mass approximation, the electron and hole eigen energies are calculated by solving the Schrodinger equation which has a form

$$\left(-\frac{\hbar^2}{2}\frac{\partial}{\partial z}\frac{1}{m_{e(h)}z}\frac{\partial}{\partial z} + V_{e(h)}(z)\right)\psi_{e(h)} = E_{e(h)}\psi_{e(h)}, \tag{1}$$

where  $E_{e(h)}$  is the electron (hole) energy, z is the electron/hole coordinate in the growth direction,  $m_{e(h)}$  is the electron (hole) effective mass,  $\psi_{e(h)}$  is the electron (hole) wave function and  $V_{e(h)}(z)$  is the electron (hole) confinement potential. The barrier layers have a potential of  $V_0$ , while the potential of tilted layers can be determined by a linear interpolation. For example, the potential of tilted layer in STQW structure is given by

$$V(z) = -\frac{V_0}{l_t} \left( z \pm \frac{l_w}{2} \right). \tag{2}$$

By substituting the tilted potential equation (2) into equation (1), in tilted layer is rewritten as

$$\frac{\partial^2 \psi(\xi)}{\partial \xi^2} - \xi \psi(\xi) = 0 \tag{3}$$

with

$$\xi = \left(\frac{2mV}{\hbar^2 L_t}\right)^{1/3} \left[ -z - \frac{L_w}{2} - \frac{EL_t}{V} \right]. \tag{4}$$

The solution of equation (3) is the combination of Airy funtions  $Ai(\xi)$  and  $Bi(\xi)$ , so that the wave function in tilted layer has a form [11]:

$$\psi(\xi) = aAi(\xi) + bBi(\xi), \tag{5}$$

where a and b are arbitrary constants.

1380 (2019) 012079 doi:10.1088/1742-6596/1380/1/012079

#### 3. Results and discussion

#### 3.1. Single tilted quantum well structure (STQW)

The electron and hole energies in STQW structure have been calculated for different structural parameters. The well width of 2-10 nm and tilted width of 1-3 nm are considered. The parameters used in this calculation are given in reference [12].

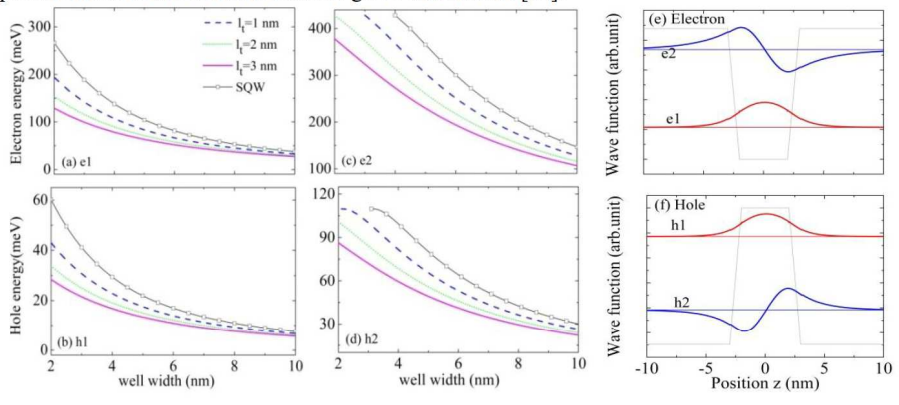


Figure 2. Electron and hole energies in STQW: (a)-(b) for the ground state (e1, h1) and (c)-(d) for the first exited state (e2, h2). The wave functions are shown in (e) for electron (f) for hole.

The results are shown in figure 2. The electron and hole energies decrease with increasing the well width. It decreases rapidly for narrow well but slightly changes for wider well. The energy level decreases as the tilted width increases as well. Again, there has been found a dramatic change in energy for small tilted width. The electron ground state energy, for example, decreases from around 260 meV to 185 meV when the tilted layer of 1 nm is inserted to the structure. However, it drops only 20 meV (from 150 meV to 130 meV) when the tilted width is increased from 2 nm to 3 nm. In addition, it is found that the hole level is lower than electron level due to a lower hole potential ( $V_0$ ) and a higher hole mass. The wave functions are also calculated in this work. The results show that the wave functions are symmetric (ground state:e1, h1) and anti-symmetric (the first excited state: e2, h2) as can be seen in figures 2 (e)-(f). The probability of finding electron (hole) in the surrounded barrier is higher in the case of e2(h2) state compared to e1(h1) state.

#### 3.2. Coupled tilted quantum well structure (CTQW)

We consider electron and hole energies level in CTQW structure. The tilted width id fixed to 1 nm and the well is width 4 nm. The barrier width is varied from 2 nm to 10 nm in order to study the effect of barrier width on the energy levels. The first four states of electron and hole as a function of barrier width are demonstrated in figure 3. As we expected, the electron and hole energies decreases when the tilted width is added to the structure. The ground energy (e1, h1) increases with increasing the barrier width, while the first excited state energy (e2, h2) decrease as the barrier width rises. This gives rise to energy splitting between e1-e2 (h1-h2) states. The splitting becomes smaller for wider barrier. At the barrier width of approximately 6 nm, the e1(h1) and e2(h2) levels tend to the same level which is the ground state level in STQW structure. This means that the two SQW act as an isolated single QW with no interaction between them. The same situation also happens in the case of e3-e4 (h3-h4) energy levels shown in figures 3 (c)-(d). The corresponding wave functions are demonstrated in figures 3(e)-(f). The singlet state in STQW becomes the doublet states with symmetric (e1, e3, h1, h3) and antisymmetric (e2, e4, h2, h4) wave functions.

1380 (2019) 012079 doi:10.1088/1742-6596/1380/1/012079

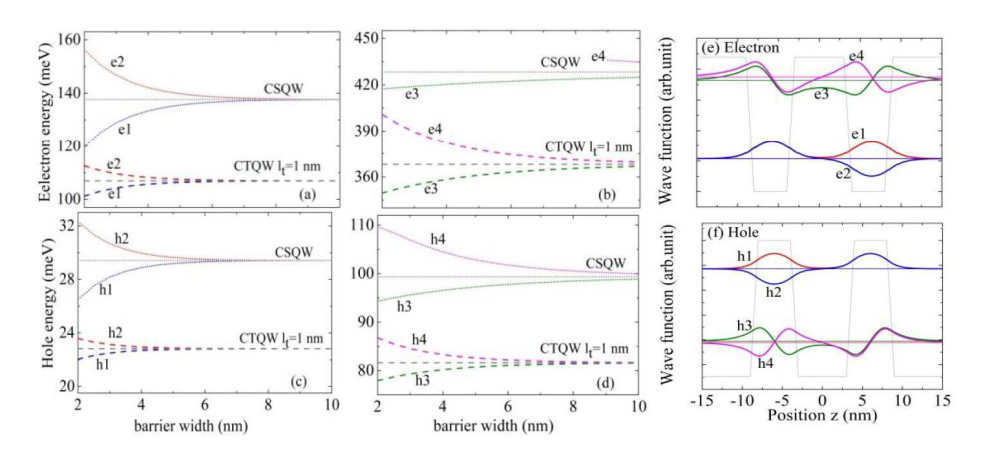


Figure 3. Electron and hole energies in CTQW for  $l_w$ =4 nm and  $l_t$ =1 nm: (a) e1-e2, (b) e3-e4,(c) h1-h2 and (d) h3-h4 states. The wave functions are shown in (e) for electron (f) for hole.

#### 4. Conclusion

In this study, the single particle states in GaInNyAs/GaAs tilted quantum well structure have been theoretically investigated by solving the Schrödinger equation in real space. It is shown that the electron and hole energies decrease with increasing the well width and tilted layer width. The wave functions are both symmetric for e1(h1) and anti-symmetric for e2(h2). The wave functions are spread out when the well width is increased. For CTQW structure, the single state is split into the doublet states. The e1(h1) energy increases but the e2(h2) energy decreases, resulting the e1-e2 (h1-h2) energy splitting. This splitting becomes smaller when the barrier increases. The energies tend to the energy level of single tilted quantum well structure (STQW); e1(h1) and e2(h2) state tend to the ground state in STQW, while e3(h3) and e4(h4) states become the first excited state in STQW. As a result, each QW acts as an isolated QW. The probability of finding electron and hole are equal in both wells.

#### Acknowledgments

The authors thank National Science and Technology Development Agency (NSTDA) and The Thailand Research Fund (TRF) for financial support.

## References

- [1] Mahala P, Singh S and Dhanavantri C 2018 Optik 166 61-8
- [2] Aissat A, Benyettou F, Nacer S and Vilcot J P 2017 Int. J. Hydrog. Energy 42 8790-4
- [3] Urabe H, Kuramoto M, Nakano T, Kawaharazuka A, Makimoto T and Horikoshi Y 2015 J. Cryst. Growth 425 330–2
- [4] Poopanya P and Sivalertporn K 2018 Phys. Lett. A 382 734-8
- [5] Yıldırım H 2018 Superlattice Microst. 114 207–13
- [6] Arulmozhi M and Anitha A 2014 Superlattice Microst. 75 222-32
- [7] Sivalertporn K 2016 Phys. Lett. A 380 1990-4
- [8] Abdalla A S, Eisa M H, Alhathlool R and Aldaghri O 2018 Optik 170 314–20
- [9] Ozturk O, Ozturk E and Elagoz S 2018 J. Mol. Struct. 1156 726–32
- [10] Grigoryev P S, Kurdyubov A S, Kuznetsova M S, Ignatiev I V, Efimov Y P, Eliseev S A, Lovteius V A and Shapochkin P Y 2016 Superlattice Microst. 97 452–62
- [11] Sivalertporn K, Mouchliadis L, Ivanov A L, Philp R and Mulijarov E A 2012 Phys. Rev. B 85 045207
- [12] Yesilgul U, Ungan F, Kasapoglu E, Sari H and Sökmen I 2015 *Physica* B **475** 110–6

**IOP Publishing** 

Journal of Physics: Conference Series

1380 (2019) 012082 doi:10.1088/1742-6596/1380/1/012082

# Effect of quantum well width on the electron and hole states in different single quantum well structures

#### N Rueangnetr and K Sivalertporn\*

Department of Physics, Faculty of Science, Ubonratchathani University, Ubonratchathani, 34190, Thailand

\*E-mail: kanchana.s@ubu.ac.th

Abstract. In this study the electron and hole states in Al<sub>0.33</sub>Ga<sub>0.67</sub>As/GaAs single quantum well structures including squared QW, step QW and tilted QW, have been theoretically studied by solving the Schrodinger equation in real space. The energies and wave functions of electron and hole are calculated for different well widths. It is found that energy level of electron and hole decreases with increasing the well width. Adding step or tilted layers gives rise to the decrease of electron and hole energy levels. The ground state energy level in a tilted single quantum well structure is lower than that in a step single quantum well structure. It is also found that the energy of electron and hole ground states do not change as the width of step layer increase. This is because the ground state occupies in a lower well only. The wave functions are symmetric (ground state) and antisymmetric (the first excited state). The maximum of ground state wave function is at the central of the well and the probability of finding electron and hole in excited states are different in each region. The hole levels are lower than the electron levels due to the lower well depth and higher mass of hole compared to electron.

#### 1. Introduction

In the past decades, the electronic and optical properties of exciton in semiconductor quantum well (QW) structure have been widely investigated because of their potential applications in optoelectronic devices. The quantum well solar cell is one of the applications which is studied in order to design the optimized solar cell with high efficiency [1-2]. The effect of structural parameters including well width, barrier width on exciton state has been theoretically studied [3-5]. The shape of potential profile is also important. Not only a squared QW but also a parabolic or triangle QW is considered [6-7]. In addition, the external field (magnetic and electric fields) has a strong effect on electron and hole states in QW [8-11].

An exciton is an electron-hole pair which is attracted to each other via the Coulomb interaction. Therefore, the electron and hole energies and wave functions in QW structure are basic quantities which is used to calculate exciton states and their properties. Here, we concentrate on the effect of potential shape on the electron and hole states. The squared, step-like and tilted QWs are studied for different parameters.

Content from this work may be used under the terms of the Creative Commons Attribution 3.0 licence. Any further distribution of this work must maintain attribution to the author(s) and the title of the work, journal citation and DOI.

Published under licence by IOP Publishing Ltd

Journal of Physics: Conference Series

**1380** (2019) 012082 doi:10.1088/1742-6596/1380/1/012082

#### 2. Method

Let us consider single quantum well structures with different potential profiles including squared QW (SQW), step-like QW (Step-QW) and tilted QW (TQW) structures. The schematic structures are shown in figure 1.

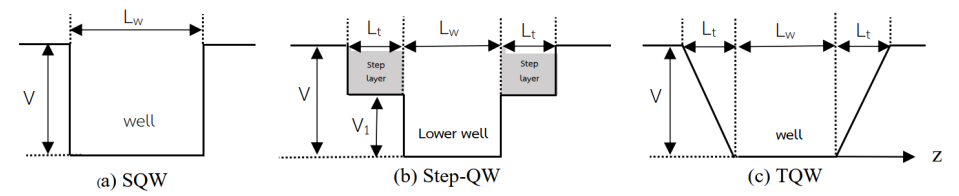


Figure 1. Schematic structures for (a) SQW (b) Step-QW (c) TQW.

Under the effective mass approximation, the electron and hole eigen energies are calculated by solving the Schrodinger equation which has form:

$$\left(-\frac{\hbar^2}{2}\frac{\partial}{\partial z}\frac{1}{m_{e(h)}z}\frac{\partial}{\partial z} + V_{e(h)}(z)\right)\psi_{e(h)} = E_{e(h)}\psi_{e(h)}$$
(1)

where  $E_{e(h)}$  is the electron (hole) energy, z is the electron/hole coordinate in the growth direction,  $m_{e(h)}$  is the electron (hole) effective mass,  $\psi_{e(h)}$  is the electron (hole) wave function, and  $V_{e(h)}$  is the electron (hole) confinement potential. The potential of step layer and surrounded barrier layer are  $V_1$  and V respectively. For SQW and Step-QW structures, the wave function in each region is given by

$$\psi_{e(h)} z = A e^{ikz} + B e^{-ikz} , \qquad (2)$$

where A and B are arbitrary constants.

For TQW structure, the potential of tilted layer is obtained by a linear interpolation and has a form

$$V(z) = -\frac{V_0}{L_t} \left( z \pm \frac{L_w}{2} \right) \tag{3}$$

By substituting the tilted potential into equation (1), the Schrodinger equation in tilted layer is rewritten as

$$\frac{\partial^2 \psi(\xi)}{\partial \xi^2} - \xi \psi(\xi) = 0, \tag{4}$$

with

$$\xi = \left(\frac{2mV}{\hbar^2 L_t}\right)^{1/3} \left[ -z - \frac{L_w}{2} - \frac{EL_t}{V} \right]$$
 (5)

The solution of equation (1) is the combination of Airy functions  $Ai(\xi)$  and  $Bi(\xi)$ , so that the wave function in tilted layer has a form [11]:

$$\psi(\xi) = CAi(\xi) + DBi(\xi) \tag{6}$$

where C and D are arbitrary constants.

1380 (2019) 012082 doi:10.1088/1742-6596/1380/1/012082

#### 3. Results and discussion

We consider the GaAs/Al<sub>x</sub>Gal<sub>1-x</sub>As QW structure with the content of x=0.33, GaAs are a well layer and AlGaAs are a barrier layer. The parameters used in the calculation are obtained from [11]. The potential  $V_1$  is set to be V/2. The squared ( $V_1$ =V/2), step and tilted quantum wells are considered in order to investigated the effect of potential profiles on the single-particle states. The structural parameters including well width ( $L_w$ =2-12 nm) and step-layer/tilted layer width ( $L_t$ =2-12 nm) are studied. The results show that the electron and hole energies in all structures decreases with increasing the well width. Figure 2 and figure 3 show the ground state and the first excited state for  $L_t$ =2, 6, 10 nm compared to the energies in SQW structure (symbol).

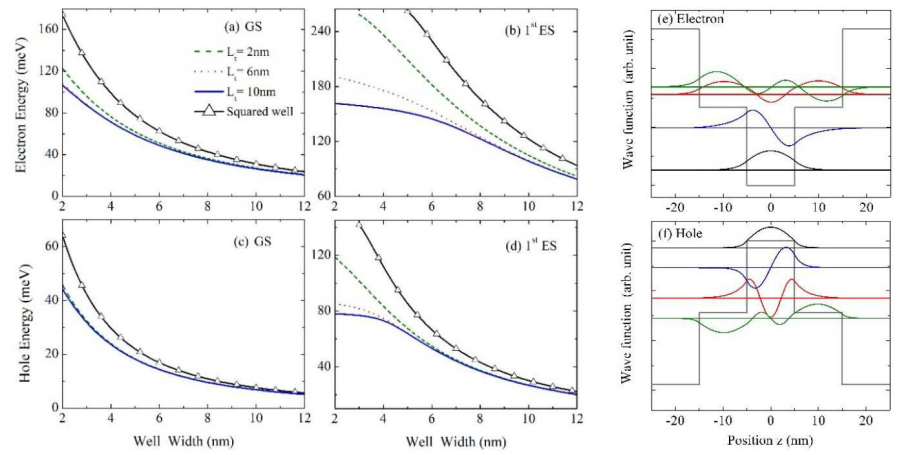


**Figure 2.** Electron and hole energies in Step-QW structure: (a),(c) for the ground state (GS) and (b),(d) for the first excited state (1stES). The wave functions are shown in (e) for electron (f) for hole.

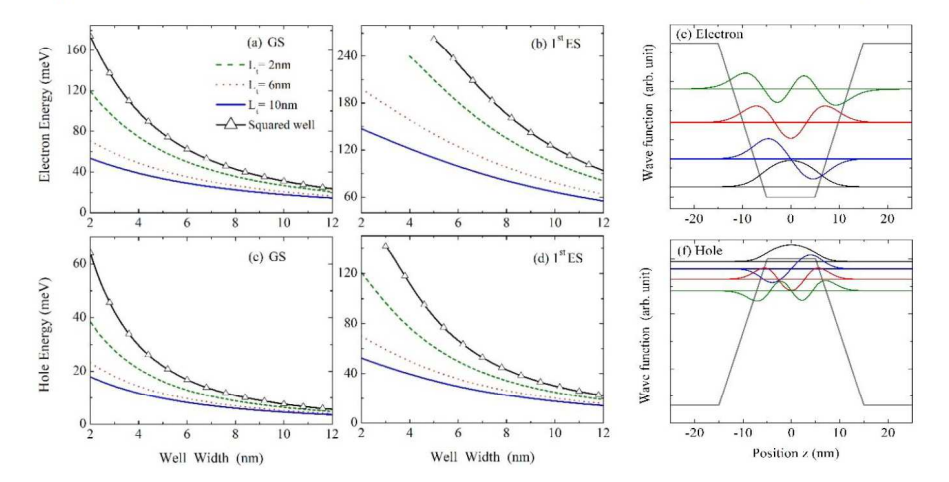


**Figure 3.** Electron and hole energies in TQW structure: (a) and (c) for the ground state (GS) and (b) and (d) for the first excited state (1<sup>st</sup>ES). The wave functions are shown in (e) for electron (f) for hole.

**1380** (2019) 012082 doi:10.1088/1742-6596/1380/1/012082

For Step-QW, there is no difference in the ground state energies (both electron and hole cases) when the step-layer width is changed. This is because the ground state electron and hole are confined in a lower well (see the wave function in figure 2(e) and (f), so that the change of step-layer width does not cause the change of ground state energy. For the first excited state the step-layer width plays an important role since the state is localized in the step layer. Noted that its energy is larger than the potential  $V_1$  ( $V_1 = 133.74$  meV for electron and  $V_1 = 72.015$  meV for hole). However, the energies for all values of  $L_t$  tend to the same level at wider well width. It happens earlier in the case of hole due to a heavier hole mass and a lower hole potential.

For TQW structure, the pictures of the ground state and the first excited state energies look similar. The electron and hole energies decrease as the tilted width increases, but a small change in energy can be observed when the tilted layer is increased from 6 nm to 10 nm. The corresponding wave functions are demonstrated in figure 3(e) and (f). It is found that the wave functions are symmetric (e1 e3 h1 h3) and antisymmetric (e2 e4 h2 h4).

#### 4. Conclusions

In this work, we calculate the electron and hole energy levels and their wave in Al<sub>0.33</sub>Ga<sub>0.67</sub>As/GaAs single quantum well structures including squared QW, step QW and tilted QW by solving the Schrodinger equation in real space. It is found that the energies of electron and hole decrease when the quantum well width and the step/tilted layer width are increased. The energy levels in the tilted QW structure smoothly change with tilted width because the potential in tilted layer is smoothly changed from the surrounded barrier potential V to the well potential. The situation is different in the case of step QW. The ground state energies of electron and hole do not change when the width of the step layer is increased. This is due to the ground state occupies in the lower well only. Therefore, the tilted layer does not affect to its energy level. The state strongly depends on the well width. The wave functions of electron and hole is both symmetric (e1 e3 h1 h3) and antisymmetric (e2 e4 h2 h4). The highest probability of finding electron (hole) is at the center of the well. In addition, it is found that the energy levels of hole is lower than the electron energy levels because of the larger hole mass and lower hole potential depth.

#### Acknowledgments

The authors thank National Science and Technology Development Agency (NSTDA) and The Thailand Research Fund (TRF) for financial support.

#### References

- [1] Mahala P, Singh S and Dhanavantri C 2018 Optik 166 61-8
- [2] Aissat A, Benyettou F, Nacer S and Vilcot J P 2017 Int. J. Hydrog. Energy 42 8790-4
- [3] Yıldırım H 2018 Superlattice Microst. 114 207–13
- [4] Arulmozhi M and Anitha A 2014 Superlattice Microst. 75 222–32
- [5] Abdalla A S, Eisa M H, Alhathlool R and Aldaghri O 2018 Optik 170 314-20
- [6] Ozturk O, Ozturk E and Elagoz S 2018 J. Mol. Struct. 1156 726–32
- [7] Grigoryev P S, Kurdyubov A S, Kuznetsova M S, Ignatiev I V, Efimov Y P, Eliseev S A, Lovtcius V A and Shapochkin P Y 2016 Superlattice Microst. 97 452–62
- [8] Khalil H M et al 2012 Mater. Sci. Eng. B 177 729–33.
- [9] Sivalertporn K 2016 Phys. Lett. A 380 1990-4
- [10] Poopanya P and Sivalertporn K 2018 Phys. Lett. A 382 734–8
- [11] Sivalertporn K, Mouchliadis L, Ivanov A L, Philp R and Mulijarov E A 2012 Phys. Rev. B 85 045207

International Journal of Nanoscience Vol. 1, No. 1 (2007) 1–7 © World Scientific Publishing Company

## Effect of step layer width and electric field on single-particle states in step quantum well structures

P. Poopanya

Program of Physics, Faculty of Science, Ubonratchathani Rajabhat University Ubon Ratchathani, 34000, Thailand.

N. Rueangnetr, W. Bukaew, K. Sivalertporn\*

Department of Physics, Faculty of Science, Ubonratchathani University

Ubon Ratchathani, 34190, Thailand.

kanchana.s@ubu.ac.th

Received Day Month Year Revised Day Month Year

The single-particle states in AlGaAs/GaAs and GaInNAs/GaAs step quantum well structures have been theoretically studied by solving straight-forwardly the Schrodinger equation in real space. The electron and hole energy levels are calculated for different well widths and step layer widths. It is found that the energies decreased with increasing the well width and step layer width, but the change is very small for a wide layer. There are two states with fews meV energy splitting observed at the energy a bit above the step potential. Therefore, these two levels can be controlled by varying the step potential. The electron and hole energies in AlGaAs/GaAs and GaInNAs/GaAs step quantum well structures are compared to that in the single squared quantum well. The results show that the energies decrease with the same trend and comparable percentage for both electron and hole cases. The ground state energy can be decreased up to nearly 50% for the step layer of  $10\,\mathrm{nm}$  at small well width. The electron and hole energies are also calculated for different applied electric fields up to  $200\,\mathrm{kV/cm}$ . The electric field can break the symmetry of the wave function and force electron and hole moving in the opposite direction which can form an indirect exciton. At large enough field, the localization of groundstate electron (hole) in the left (right) step layer is maximum due to the tilted potential which is correspond to the anticrossing at around  $130\,\mathrm{meV}$  for electron and  $70\,\mathrm{meV}$  for hole in the field dependence of energy profile.

Keywords: step quantum wells single-particle state step layer width.

## 1. Introduction

The semiconductor quantum well (QW) heterostructures have been attracted much attention for few decades due to their potential applications in optoelectronic devices such as laser diodes  $^{1,\ 2}$ , photodetectors  $^3$  and solar cell  $^{4-6}$ . The electrical and

optical properties of exciton in QW structure have been experimentally and theoretically studied in order to understand the fundamental physics and improve the efficiency of the electronic devices <sup>7, 8</sup>. The exciton energy level can be controlled by varying the well width, potential height or external electric

<sup>\*</sup>Corresponding author

#### 2 P. Poopanya et. al.

field applied in the growth direction. As a result, the effect of these parameters on electron, hole and exciton states have been theoretically investigated in order to improve the device efficiency 9-14. The conversion efficiency of GaN/InGaN multi quantum well (MQW) solar cell have been calculated for different structural parameters such as thickness, potential and number of QW layers. The results can be used to design and interprete the characteristic of optimized MQW solar cell 15. The optical property of InGaN laser diodes have been studied for different well thickness to obtain the best design for laser diode  $^{16}$ . It is found that the optical gain is large if a QW thickness is small because the carriers are confined and localized in a small QW. Not only the well width is important, but the shape of potential profile is also a significant parameter. Different shapes give rise to different electronic property of the device  $^{17-19}$ . There are several studies focus on the double QW structure which consists of two QWs separated by a thin barrier layer  $^{20-22}$ . One interesting point is that the indirect exciton (an electron and a hole are in different well) can be formed when the electric field is applied in such structure <sup>23</sup>. The indirect exciton has a longer lifetime and larger binding energy compared to the direct exciton in a single QW structure. Recently, it has been reported that the spin relaxation time of indirect exciton is 100 times larger than that of direct exciton 24. The tunneling effect can also be enhanced at large electric field allowing the carrier to leak out of the system <sup>25–28</sup>. In addition, the interaction of exciton and photon has also been investigated when the quantum well structure is placed in the microcavity. The strong and weak coupling regimes are demonstrated and can be controlled by the electric field <sup>29</sup> or magnetic field <sup>30, 31</sup>.

In this work, we concentrate on AlGaAs/GaAs and GaInNAs/GaAs step QW structures in order to study the effect of step layer on the electron and hole states. The former structure is used in various electronics and photoelectronic devices, while the latter structure have been attracting great interest due to their direct and large band gap which is appropriate for short wavelength devices. The dilute nitride III-V compound semiconductor has a wide range of band gap varied from 0.64 eV (InN) to 3.4 eV (GaN). Therefore, it is suitable for solar cell applications as well. The single-particle states in step potential profile have been studied for different structural parameters and applied electric field.

The results are compared to the single QW state to see how the energy level changes.

#### 2. Theoretical Model

Let us consider a symmetric QW structure consisting of a QW layers sandwiched between two step layers with the width  $L_t$ . The system is surrounded on both sides by thick barriers with wider band gap (Fig.1). The step potential  $V_1$  is set to be lower than the surrounded potential V to make a step-like QW.

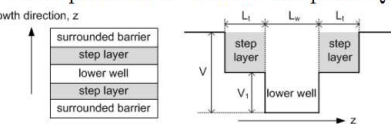


Fig. 1. Schematic of step QW structure.

Under the effective mass approximation, the electron and hole eigen energies are calculated by solving the Schrodinger equation which has a form:

$$\left(-\frac{\hbar^2}{2}\frac{\partial}{\partial z}\frac{1}{m_{e(h)}}\frac{\partial}{\partial z} + \mathbf{V}_{e(h)}(z)\right)\psi_{e(h)} = E_{e(h)}\psi_{e(h)},\tag{1}$$

where  $E_{e(h)}$  is the electron (hole) energy, z is the electron/hole coordinate in the growth direction,  $m_{e(h)}$  is the electron (hole) effective mass and  $\mathbf{V}_{e(h)}$  is the electron (hole) confinement potential which has a step-like profile:

$$\mathbf{V}_{e(h)}(z) = \begin{cases} 0, & |z| \le L_w/2 \\ V_{1,e(h)}, & L_w/2 \le |z| \le L_w/2 + L_t \\ V_{e(h)}, & |z| \ge L_w/2 + L_t \end{cases}$$

The single-particle wave functions  $\psi_{e(h)}(z)$  satisfying the Schrodinger equation is a combination of two exponential terms (incoming and outgoing parts).

In the presence of electric field, the Schrödinger equation including the potential due to the electric field is given by

$$\left(-\frac{\hbar^2}{2}\frac{\partial}{\partial z}\frac{1}{m}\frac{\partial}{\partial z} + \mathbf{V} \pm eFz\right)\psi = E\psi, \quad (2)$$

and can be rewritten in a form

$$\frac{d^2\psi}{d\xi^2} - \xi\psi = 0,\tag{3}$$

with

$$\xi = \left(\frac{2mF}{\hbar^2}\right)^{1/3} \left(z + \frac{\mathbf{V} - E}{F}\right). \tag{4}$$

funcions:

The solution of Eq. (3) is the combination of Airy

$$\psi(\xi) = aAi(\xi) + bBi(\xi), \tag{5}$$

where a and b are an arbitrary constant. The detail of the model is explained in Ref.  $^{23}$ .

#### 3. Results and Discussion

We consider  $Al_xGa_{1-x}As/GaAs$  (with x=0.33) and  $Ga_{1-x}In_xN_yAs_{1-y}/GaAs$  (with x=0.35, y=0.005) step QW structures in order to study the effect of structural parameters on electron and hole energies. A QW layer has narrow band gap, while a wider band gap material is used as a surrounded barrier. The step layer material is the same material as the surrounded layer but has different x and y contents. The parameters for the step layer are calculated by linear interpolation between the well layer and barrier layer. The well width and step layer width are veried from  $0.1\,\mathrm{nm}$  to  $12\,\mathrm{nm}$ . The parameters for electron/hole mass and potential are shown in Table. 1. The mass  $m_1$ ,  $m_2$  and  $m_3$  are the mass in well layer, barrier layer and step layer respectively.

Table 1. Parameters used in the calculation.

parameter	${\rm AlGaAs/GaAs}^{23}$	${ m GaInNAs/GaAs}^{32}$
$V_e \text{ (meV)}$	267.48	438.83
$V_h \text{ (meV)}$	144.03	109.70
Well layer	GaAs	GaInNAs
$m_{1,e}(m_0)$	0.0665	0.0656
$m_{1,h}({ m m}_0)$	0.34	0.3447
barrier layer	AlGaAs	GaAs
$m_{2,e}({ m m}_0)$	0.0941	0.0665
$m_{2,h}(m_0)$	0.476	0.34

#### 3.1. Structural Dependence

The electron and hole energies in AlGaAs/GaAs step QW structure with different step layer widths are calculated as a function of well width (Fig. 2). The energies for all cases decrease with increasing the well width. Adding the step layer gives rise to the decrease of electron and hole energies compared to the single squared well structure. For the ground state (GS), the energy of electron (hole) rapidly drops from 265 meV (142 meV) in single squared well to 200 meV (90 meV) in the case of 2-nm step layer. However, the energy changes very small when the step layer is increased from 6-nm to 10-nm.

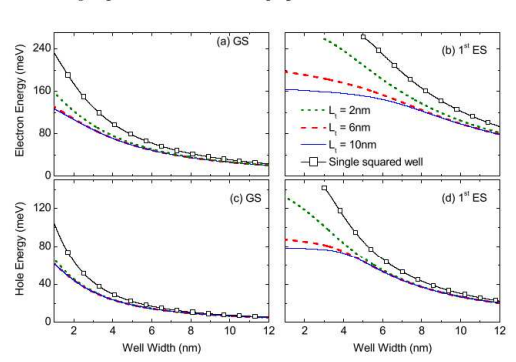


Fig. 2. Ground state (GS) and the first excited state ( $1^{st}$  ES) energies in AlGaAs/GaAs step QW structure as a function of well width for  $L_t$ =2 nm (solid), 6 nm (dashed) and 10 nm (dotted): (a)-(b) for electron and (c)-(d) for hole. The symbols indicate the energy level in AlGaAs/GaAs single squared well.

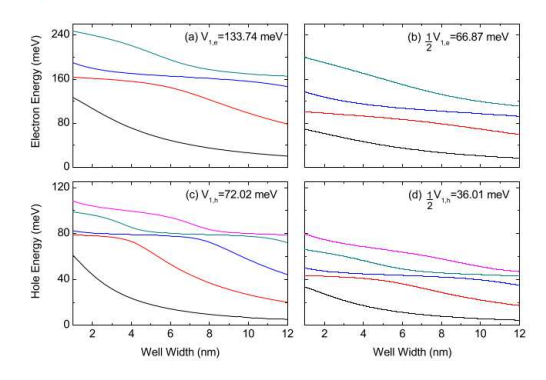


Fig. 3. Four states of electron and five states of hole in Al-GaAs/GaAs step QW structure for  $L_t{=}10\,\mathrm{nm}$  and different step potential as a function of well width: (a) for electron with  $V_{1,e}{=}133.74\,\mathrm{meV},$  (b) for electron with  $\frac{1}{2}V_{1,e}{=}66.87\,\mathrm{meV},$  (c) for hole with  $V_{1,h}{=}72.02\,\mathrm{meV},$  and (d) for hole with  $\frac{1}{2}V_{1,h}{=}36.01\,\mathrm{meV}.$ 

It is clearly seen from Fig. 2(a) and Fig. 2(c) that the electron and hole energies in 10-nm step QW are very close to that of 6-nm step layer case. Only a small difference is observed at a narrow well width. The reason is that all these energies are lower than the step potential  $(V_{1,e}=133.74\,\mathrm{meV}$  for electron and  $V_{1,h}=72.02\,\mathrm{meV}$  for hole) residing in the lower QW, so that the change of step layer width does not affect to these energy levels. At approximately  $L_w=6\,\mathrm{nm}$  ( $L_w=2\,\mathrm{nm}$ ), the electron (hole) energies in step QW for all cases are the same at the energy of around 60 meV (40 meV). It is observed at a narrower well in the case of hole because of

#### 4 P. Poopanya et. al.

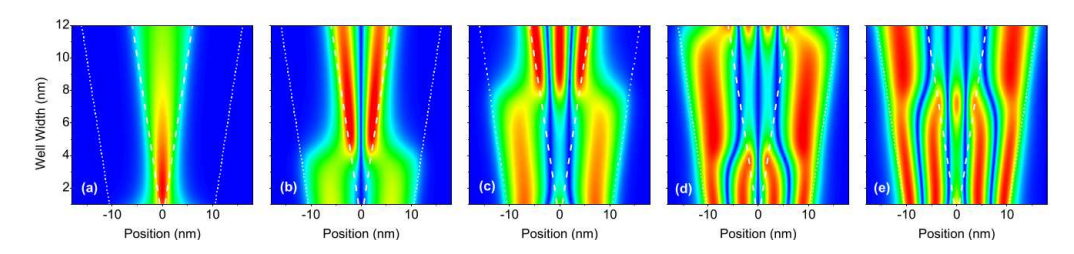


Fig. 4. 2D Wave functions of five hole state in AlGaAs/GaAs step QW structure for  $L_t$ =10 nm: (a) GS, (b)  $1^{st}$  ES, (c)  $2^{nd}$ ES, (d) 3<sup>rd</sup> ES, and (e) 4<sup>th</sup> ES states. The x-axis is the position in z direction and y-axis is the well width up to 12 nm. The region inside two white dashed lines is the lower well region, while two white dotted lines indicate the step layer edges.

the heavier mass and lower potential of hole. For the first excited state  $(1^{st}ES)$  [Fig.2(b), (d)], it is also observed a large difference in energy between 2-nm and 6-nm cases and only a small change between 6-nm and 10-nm of step layer. Again, when the energies are lower than the potential  $V_1$  which means that the state already occupies in the lower well. The step layer has no longer influence on the energy and all levels tend to the same level.

Figure 3 shows the electron and hole energies in a 10-nm step QW structure (four states of electron and five states of hole). It is notices that there are excited states lie parallel at the energy of approximately 160 meV for electron and 80 meV for hole which are near the bottom of the step potential. The hole energy in Fig. 3(c) shows that the first excited state energy remains unchange at 80 meV at  $L_w=1$  nm, while the second excited state starts at around 95 meV and decreases to 80 meV. The second excited state then remains at this level and parallel to the first excited state for  $L_w < 4$ . When  $L_w>4$  nm the first excited state drops down to lower energy, the third excited state comes to the level of 80 meV and is parallel to the second excited state for the well width of  $L_w=5-8\,\mathrm{meV}$ . The same also happens for the fourth excited state and so on. The energy splitting of two paralleling states is about 10 meV for electron and 3 meV for hole. The step potential  $V_1$  is decreased by a factor of two in order to see how the electron and hole energies change [fig. 3(b),(d)]. It is found that the energy trend does not change, the calculated energies only shift down to lower energy due to a lower potential. There also be two paralleling energy levels at the energy which is above the step potential  $V_1/2$ . The splitting between the two energies is twice compared to the case of  $V_1$  step potential. The hole wave functions

of five states in AlGaAs/GaAs step QW strucuture are demonstrated in Fig. 4. The white dashed lines indicate the region inside the lower well, while the while dotted lines show the edge of the step layer. It is found that there are two broadening peaks in the step well region when the excited state remains at the parallel level ( $L_w < 4 \,\mathrm{nm}$  for 1st ES,  $L_w$  <8 nm for 2nd ES, 4< $L_w$  <11 nm for 3rd ES and  $L_w > 8 \,\mathrm{nm}$  for 4th ES). As we know, the Nth excited state should has N maxima of the wave function. However, all peaks in the middle always very small compared to the two broadening peaks. The sharp peaks inside the well region in Fig. 4(b) for  $L_w>4$  nm and in Fig. 4(c) for  $L_w>8$  nm are observed when hole energy drops down to the level below the step potential, corresponding to a strongly decrease of energy as the well width increases in Fig. 3.

We have also calculated the electron and hole energies in the GaInNAs step QW structure (Fig. 5). The parameters used in the calculation are shown in Table. 1. The results show that the well width dependence of energies looks very similar to those in AlGaAs/GaAs step QW structure. In order to understand in more details, we have calculated the difference of electron and hole energies in the step QW  $(E_{step})$  compared to their energies in the single squared QW ( $E_{squared}$ ) and calculate their percentage by

$$\Delta E = E_{squared} - E_{step},\tag{6}$$

$$\Delta E = E_{squared} - E_{step}, \tag{6}$$

$$\% E = \frac{\Delta E}{E_{squared}} \times 100, \tag{7}$$



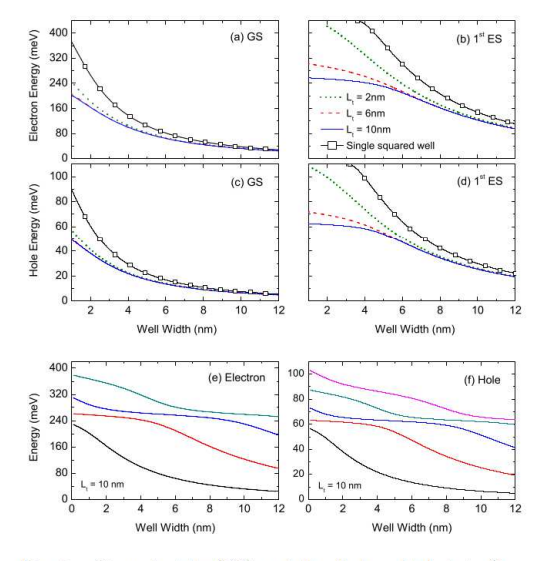


Fig. 5. Ground state (GS) and the first excited state ( $1_{st}$ ES) energies in GaInNAs/GaAs step QW structure as a function of well width for  $L_t=2 \,\mathrm{nm}$  (solid),  $6 \,\mathrm{nm}$  (dashed) and 10 nm (dotted): (a),(b) for electron and (c),(d) for hole. The symbols indicate the energy level in AlGaAs/GaAs single squared well. The four states of electron (e) and five states of hole (f) for  $L_t=10\,\mathrm{nm}$  are calculated as a function of well width

Figure 6 shows the decreasing rate of ground state energy in AlGaAs/GaAs and GaInNAs/GaAs step QW structures as a function of well width. The percentages of energy difference exhibit the similar trend for both electron and hole. The ground state energy can be reduced up to nearly 50% for 10nm step layer width and a narrow well width. For a wider well width, the decreasing rates are satuarated at about 10% for all values of step layer. This is because the step layer width does not influence on the ground state energy as discussed before.

#### 3.2. Electric Field Dependence

When the electric field is applied to the structure in the growth direction, the potential profile is tilted as shown in Fig. 7. The electron and hole energies are calculated for the electric field up to 200 kV/cm and the step layer width is fixed at  $L_t=10 \text{ nm}$ . The results show that the ground state energy remains nearly constant at low electric field and the energies then linearly decrease with increasing field giving rise to an anticrossing in energy (Fig. 8).

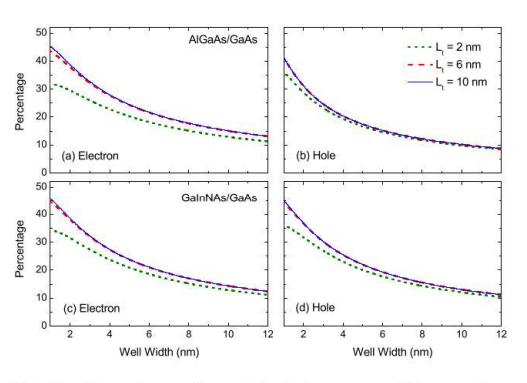


Fig. 6. Percentage of ground state energy difference between the step QW and single squared QW for (a)-(b) Al-GaAs/GaAs and (c)-(d) GaInNAs/GaAs structures

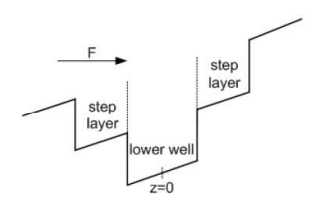


Fig. 7. Potential profile in the presence of electric field.

This anticrossing happens at larger field for wider well width. The first four energy states of electron and hole for  $L_t=8\,\mathrm{nm}$  are demonstrated in Fig. 8(c)-(d). The anticrossing of GS-1 $^{st}$ ES energy happens at around  $F=130\,\mathrm{kV/cm}$  for electron and  $F=75\,\mathrm{kV/cm}$  for hole. The electron wave functions at  $F=120 \,\mathrm{kV/cm}$  (before the electron anticrossing) and  $F=140\,\mathrm{kV/cm}$  (after the electron anticrossing) in Fig. 8(e) show that the maximum of the wave function changes from the well layer to step layer. The reason why electron is now confined in the step layer after the anticrossing is because the large field makes the step layer potential becomes lower than the well potential. Moreover, the tilted potential due to the electric field can cause the tunneling of electron/hole through the surrounded barrier which can be observed the oscillation in the left region as shown in Fig. 8(e). A larger field leads to a larger tunneling effect.

#### 6 P. Poopanya et. al.

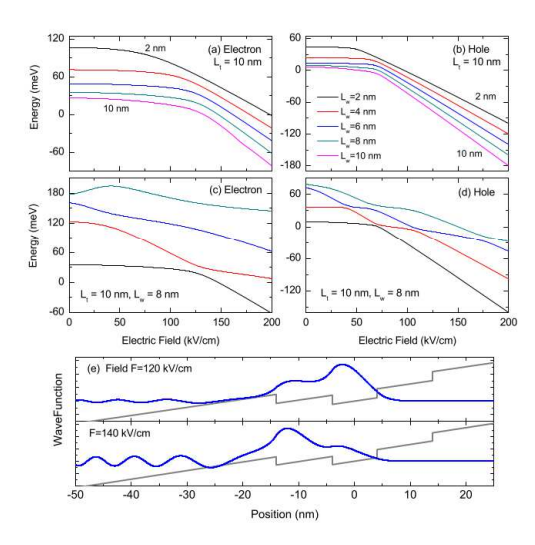


Fig. 8. Electric field dependence of electron and hole energy in AlGaAs/GaAs step QW structure: (a)-(b) showing the GS energy for different step layer widths  $L_t$ , (c)-(d) demonstrating four energy levels for  $L_t=10$  nm and  $L_w=8$  nm. The anticrossing of electron energy is observed at around 130 kV/cm. The wave functions of electron ground state at F=120 kV/cm (before the anticrossing) and F=140 kV/cm (after the anticrossing) are demonstrated in (e).

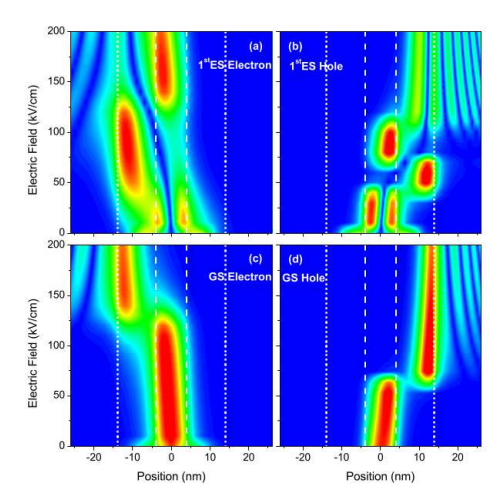


Fig. 9. 2D Wave functions of electron and hole in Al-GaAs/GaAs step QW structure for  $L_t = 10 \, \mathrm{nm}$  and  $L_w = 8 \, \mathrm{nm}$ : (a)-(b) for  $1_{st}$  ES, (c)-(d) for GS. x-axis is the position in z direction and y-axis is the electric field up to  $200 \, \mathrm{kV/m}$ . The region inside two dashed lines is the lower well region, while dotted lines indicate the step layer edges.

The electron and hole wave functions for  $L_t=10 \,\mathrm{nm}$  and  $L_w=8 \,\mathrm{nm}$  are plotted as a function of electric field (Fig. 9). Electron and hole ground states are not confined at the center anymore. Electron moves to the left and hole moves to the right due to the electric field. The wave function maxima of electron (hole) are observed at the left (right) wall. The change of wave function localization occurs at the energy anticrossing. After the anticrossing, the ground state electron locates in the left step layer, while the first excited state electron is confined in the well layer instead. The same situation also happens in the case of hole, but hole will move to the right. Note that ground state electron is in the left step layer and ground state hole resides in the right step layer at large field, so that it is possible to form an indirect exciton in the step QW structure.

#### 4. Conclusion

The electron and hole energies and wave functions in step QW structures have been calculated for different well width and step layer width. We consider AlGaAs/GaAs and GaInNAs/GaAs structures in order to study the effect of mass and potential height on electron and hole energies. It is found that the energies in AlGaAs/GaAs and GaInNAs/GaAs step QWs decrease with comparable percentage compared to their own single squared well level. The trends for electron and hole are similar. This means that we can predict the electron and hole energies in any step QWs from their single QW structures. With no electric field, the wave functions are symmetric and the probability of finding ground state electron (hole) is maximum at the center of the well. The well width dependence of energy shows the two excited state energies lie parallel to each other at the energy near a bottom of step layer. The wave function of these two states has its maxima at the center of step layers with a broadening peak.

In the presence of the electric field, the symmetry of the system is broken and the potential is tilted. As a result, electron move to the left and hole move to the right due to the field creating an indirect exciton. The GS-1<sup>st</sup>ES anticrossing happens when the electric field is large enough to make the step potential is lower than the well potential. The GS electron (hole) after the anticrossing is confined in a left (right) step layer, while the 1<sup>st</sup>ES electron (hole) localization changes from a left(right) step layer to well layer. Finally, the calculated re-

sults show that the step layer width and potential height, and the electric field has a significant effect on the electron and hole states which are related to the electrical and optical properties of exciton. The results are also compared to the case of single squared well. Therefore, these results can be used to understand the experimental data design the optimized devices.

#### Acknowledgements

The author thanks National Science and Technology Development Agency (NSTDA) and The Thailand Research Fund (TRF) for financial support.

#### References

- A. Tiutiunnyk, M.E. Mora-Ramos, A.L. Morales, C.M. Duque, R.L. Restrepo, F. Ungan, J.C. Martnez-Orozco, E. Kasapoglu, C.A. Duque, Opt. Mater. 64 (2017) 496.
- S. Dehimi, L. Dehimi, T. Asar, B. Mebarki, S. zelik, Optik 135 (2017) 153.
- A. Albo, D. Fekete, G. Bahir, Infrared phys. Techn. 96 (2019) 68.
- H. M. Khalil, S. Mazzucato, S. Ardali, O. Celik, S. Mutlu, B. Royall, E. Tiras, N. Balkan, J. Puustinen, V.-M. Korpijrvi, M. Guina, Mater. Sci. Eng. B 177 (2012) 729.
- N.Miyashita, N.Ahsan, Y.Okada, Sol. Energ. Mat. Sol. C. 111 (2013) 127.
- H. Urabe, M. Kuramoto, T. Nakano, A. Kawaharazuka, T. Makimoto, Y. Horikoshi, J. Cryst. Growth 425 (2015) 330.
- R. L. Restrepo, J. P. Gonzlez-Pereira, E. Kasapoglu, A. L. Morales, C. A. Duque, Opt. Mater. 86 (2018) 590.
- P. S. Grigoryev, A. S. Kurdyubov, M. S. Kuznetsova, I. V. Ignatiev, Yu. P. Efimov, S. A. Eliseev, V. V. Petrov, V. A. Lovtcius, P. Yu. Shapochkin, Superlattices Microstruct. 97 (2016) 452.
- M. Miyoshi, T. Tsutsumi, T. Kabata, T. Mori, T. Egawa, Solid State Electron. 129 (2017) 29.
- J. Zhu, S.L. Ban, S.H. Ha, Superlattices Microstruct. 56 (2013) 92.
- Z. Gu, Z. N. Zhu, M. M. Wang, Y. Q. Wang, M. S. Wang, Y. Qu, S. L. Ban, Superlattices Microstruct. 102 (2017) 391-398.

- S. Dietrich, J. Kanter, W. Mayer, S. Vitkalov, D. V. Dmitriev, A. A. Bykov, Phys. Rev. B 92 (2015) 155411.
- Z.-H. Zhang, L. Zou, C. Liu, J.-H. Yuan, Superlattices Microstruct. 85 (2015) 385.
- P. Poopanya and K. Sivalertporn, Phys. Lett. A 382 (2018) 734.
- P. Mahala, S. Singh, C. Dhanavantri, Optik 166 (2018) 61.
- 16. R. A. Abdullah, K. Ibrahim, Optik 124 (2013) 292.
- 17. K. Ryczko, G. Sek, Opt. Mater. 88 (2019) 252.
- E. Kasapoglu, C. A. Duque, M. E. Mora-Ramos,
   R. L. Restrepo, F. Ungan, U. Yesilgul, H. Sari, I.
   Sökmen, Mater. Chem. Phys. 154 (2015) 170.
- O. Ozturk, E. Ozturk, S. Elagoz, J. Mol. Struct. 1156 (2018) 726.
- U. Yesilgul, E. B. Ali, J. C. Martinez-Orozco, R. L. Restrepo, M. E. Mora-Ramos, C. A. Duque, F. Ungan, E. Kasapoglu, Opt. Mater. 58 (2016) 107.
- F. Ungan, U. Yesilgul, S. Sakiroglu, E. Kasapoglu,
   H. Sari, I. Sökmen, J. Lumin. 143 (2013) 75.
- K. Sivalertporn, Phys. Lett. A 380 (2016) 1990.
- K. Sivalertporn, L. Mouchliadis, A.L. Ivanov, R. Philp, E.A. Muljarov, Phys. Rev. B 85 (2012) 045207.
- P. Andreakou, S. Cronenberger, D. Scalbert, A. Nalitov, N. A. Gippius, A. V. Kavokin, M. Nawrocki, J. R. Leonard, L. V. Butov, K. L. Campman, A. C. Gossard, M. Vladimirova, Phys. Rev. B 91 (2015) 125437.
- J. E. Golub, K. Kash, J. P. Harbison, L. T. Florez, Phys. Rev. B 41 (1990) 8564.
- A. Alexandrou, J. A. Kash, E. E. Mendez, M. Zachau, J. M. Hong, T. Fukuzawa, Y. Hase, Phys. Rev. B 42 (1990) 9225.
- 27. D. Ahn, S. L. Chuang, Phys. Rev. B 34 (1986) 9034.
- E. J. Austin, M. Jaros, Appl. Phys. Lett. 47 (1985) 274.
- K. Sivalertporn, E. A. Muljarov, Phys. Rev. Lett. 115 (2015) 077401.
- J. Wilkes, E. A. Muljarov, Phys. Rev. B 94 (2016) 125310.
- J. Wilkes, E. A. Muljarov, Superlattices Microstruct. 108 (2017) 32.
- U. Yesilgul, F. Ungan, E. Kasapoglu, H. Sari, I. Sökmen, Phys. B 407 (2012) 528.

4) we attended to the SPC2019 conference and submitted the special project of undergraduated students which is the part of the reserch project to the conference competition. Our work passed through the final round of the compitition.







## ประกาศรายชื่อผู้ผ่านการเข้ารอบชิงชนะเลิศ การประกวดโครงงานระดับปริญญาตรีสาขาวิชาฟิสิกส์ ชิงถ้วยพระราชทาน สมเด็จพระเจ้าพี่นางเธอเจ้าฟ้ากัลยาณิวัฒนา กรมหลวงนราธิวาสราชนครินทร์

1. นางสาวสุธาวี อิทธิพงศ์เมธี มหาวิทยาลัยเทคโนโลยีพระจอมเกล้าธนบุรี 2. นายศุภโชค บัวรักษ์ มหาวิทยาลัยสงขลานครินทร์ 3. นายฐปนัท เสมอจิตร์ มหาวิทยาลัยเทคโนโลยีพระจอมเกล้าธนบุรี 4. นายณัฏฐกันย์ เรื่องเนตร มหาวิทยาลัยอุบลราชธานี มหาวิทยาลัยมหิดล 5. Mr.Supalert Sukrakarn 6. Mr.Jirawat Saipet มหาวิทยาลัยมหิดล มหาวิทยาลัยมหาสารคาม 7. นายกฤษณะ สุวรรณา 8. นายนายพงษ์เทพ วงษ์ศิริ จุฬาลงกรณ์มหาวิทยาลัย 9. นางสาวขัตติยา ช่วยยิ้ม มหาวิทยาลัยธรรมศาสตร์ 10. นายอภิรักษ์ จุลศรี มหาวิทยาลัยราชภัฏมหาสารคาม 11. Miss.Charin Seesomdee จุฬาลงกรณ์มหาวิทยาลัย